PB82-229287

Atmospheric Releases from Standardized Nuclear Power Plants: A Wind Tunnel Study

(U.S.) Environmental Sciences Research Lab.
Research Triangle Park, NC

Apr 82

U.S. Department of Commerce
National Technical Information Service
NTIS

TECHNICAL REPORT DATA (Please read Instructions on the reverse before completing)		
1. REPORT NO. EPA-600/3-82-035	2.	3. RECIPIENT'S ACCESSION NO. PB82 229287
4. TITLE AND SUBTITLE ATMOSPHERIC RELEASES FROM STANDARDIZED NUCLEAR POWER PLANTS A Wind Tunnel Study		5. REPORT DATE April 1982 6. PERFORMING ORGANIZATION CODE
7. AUTHOR(S) Al W. Payne and William H. Snyder		8. PERFORMING ORGANIZATION REPORT NO. Fluid Modeling Report No. 12
9. PERFORMING ORGANIZATION NAME AND ADDRESS Environmental Sciences Research Laboratory Office of Research and Development U.S. Environmental Protection Agency Research Triangle Park, NC 27711		10. PROGRAM ELEMENT NO. CDTA1D/03-1313 (FY-81) 11. CONTRACT/GRANT NO.
12. SPONSORING AGENCY NAME AND ADDRESS Environmental Sciences Research Laboratory - RTP, NC Office of Research and Development U.S. Environmental Protection Agency Research Triangle Park, NC 27711		13. TYPE OF REPORT AND PERIOD COVERED In-house 14. SPONSORING AGENCY CODE EPA/600/09
15. SUPPLEMENTARY NOTES		

16. ABSTRACT

Laboratory experiments were conducted to simulate radiopollutant effluents released to the atmosphere from two standard design nuclear power plants. The main objective of the study was to compare the dispersion in the wake of the standardized nuclear power plants with that in a simulated atmospheric boundary layer.

A large meteorological wind tunnel was used to simulate a suburban atmospheric boundary layer. The model-prototype scale was 1:300 and the roughness length was approximately 1.0 m full scale. The model boundary layer simulated full scale dispersion from ground level and elevated release points over surfaces of comparable roughness length.

Dispersion functions were determined that described the effluent plume spread in the wake of each nuclear plant. The dispersion functions were described by power laws. The functions were determined for three incident wind angles and the number of stacks associated with each nuclear plant. Lateral plume spread was directly related to the silhouette area of the nuclear plant. A graphical technique was developed to determine a lateral dispersion function related to the associated silhouette area of a building or building complex.

17. KEY WORDS AND DOCUMENT ANALYSIS		
a. DESCRIPTORS	b. IDENTIFIERS/OPEN ENDED TERMS	c. COSATI Field/Group
18. DISTRIBUTION STATEMENT RELEASE TO PUBLIC	19. SECURITY CLASS (This Report) UNCLASSIFIED 20. SECURITY CLASS (This page) UNCLASSIFIED	21. NO. OF PAGES 70 22. PRICE

EPA Form 2220-1 (9-73)

United States
Environmental Protection
Agency

Environmental Sciences Research
Laboratory
Research Triangle Park NC 27711

EPA-600/3-82-035
April 1982

Research and Development

PB82-229287

EPA

Atmospheric Releases from Standarized Nuclear Power Plants

A Wind Tunnel Study

REPRODUCED BY
NATIONAL TECHNICAL
INFORMATION SERVICE
U.S. DEPARTMENT OF COMMERCE
SPRINGFIELD, VA 22161

RESEARCH REPORTING SERIES

Research reports of the Office of Research and Development, U.S. Environmental Protection Agency, have been grouped into nine series. These nine broad categories were established to facilitate further development and application of environmental technology. Elimination of traditional grouping was consciously planned to foster technology transfer and a maximum interface in related fields. The nine series are:

1. Environmental Health Effects Research
2. Environmental Protection Technology
3. Ecological Research
4. Environmental Monitoring
5. Socioeconomic Environmental Studies
6. Scientific and Technical Assessment Reports (STAR)
7. Interagency Energy-Environment Research and Development
8. "Special" Reports
9. Miscellaneous Reports

This report has been assigned to the ECOLOGICAL RESEARCH series. This series describes research on the effects of pollution on humans, plant and animal species, and materials. Problems are assessed for their long- and short-term influences. Investigations include formation, transport, and pathway studies to determine the fate of pollutants and their effects. This work provides the technical basis for setting standards to minimize undesirable changes in living organisms in the aquatic, terrestrial, and atmospheric environments.

This document is available to the public through the National Technical Information Service, Springfield, Virginia 22161.

EPA-600/3-82-035
April 1982

Atmospheric Releases from Standarized Nuclear Power Plants

A Wind Tunnel Study

by

Al W. Payne
and
William H. Snyder

Meteorology and Assessment Division
Environmental Sciences Research Laboratory
U.S. Environmental Protection Agency
Research Triangle Park, North Carolina 27711

and

James E. Watson, Jr.

Department of Environmental Sciences and Engineering
School of Public Health
The University of North Carolina
Chapel Hill, North Carolina 27514

ENVIRONMENTAL SCIENCES RESEARCH LABORATORY
OFFICE OF RESEARCH AND DEVELOPMENT
U.S. ENVIRONMENTAL PROTECTION AGENCY
RESEARCH TRIANGLE PARK, NORTH CAROLINA 27711

April 1982

DISCLAIMER

This report has been reviewed by the Environmental Sciences Research Laboratory, U.S. Environmental Protection Agency, and approved for publication. Approval does not signify that the contents necessarily reflect the views and policies of the U.S. Environmental Protection Agency, nor does mention of trade names or commercial products constitute endorsement or recommendation for use.

AFFILIATION

Al W. Payne and William H. Snyder were physical scientists in the Meteorology and Assessment Division, Environmental Sciences Research Laboratory, U.S. Environmental Protection Agency, Research Triangle Park, NC. They were on assignment from the National Oceanic and Atmospheric Administration, U.S. Department of Commerce.

ABSTRACT

Laboratory experiments were conducted to simulate radiopollutant effluents released to the atmosphere from two standard design nuclear power plants. The main objective of the study was to compare the dispersion in the wake of the standardized nuclear power plants with that in a simulated atmospheric boundary layer.

A large meteorological wind tunnel was used to simulate a suburban atmospheric boundary layer. The model-prototype scale was 1:300 and the roughness length was approximately 1.0 m full scale. The model boundary layer simulated full scale dispersion from ground level and elevated release points over surfaces of comparable roughness length.

Dispersion functions were determined that described the effluent plume spread in the wake of each nuclear plant. The dispersion functions were described by power laws. The functions were determined for three incident wind angles and the number of stacks associated with each nuclear plant. Lateral plume spread was directly related to the silhouette area of the nuclear plant. A graphical technique was developed to determine a lateral dispersion function related to the associated silhouette area of a building or building complex.

CONTENTS

ABSTRACT iii
FIGURES vi
TABLES ix
SYMBOLS x

1. INTRODUCTION 1

2. CONCLUSIONS 3

3. EXPERIMENTAL EQUIPMENT AND PROCEDURES 5
The meteorological wind tunnel 5
Design of the experiment 5
Similarity criteria 7
Wind tunnel arrangement 8
Isolated stack model (STACK) 10
Standard nuclear unit power plant system model (SNUPPS) 10
Standard reactor island design model (STRIDE) 13
Flow visualization 16
Velocity measurements 17
Concentration measurements 17
Simulation of suburban atmospheric boundary layer 19

4. RESULTS AND DISCUSSION 21
The suburban boundary layer 21
Velocity measurements 21
Dispersion characteristics of the boundary layer 25
Flow visualization 40
Building wake effects 40
Building wake corrections 44
Building wake functions for SNUPPS and STRIDE 44
Normalization of derived wake functions 52

REFERENCES 58

FIGURES

NUMBER	TITLE	PAGE
1.	Overall plan and elevation of the EPA Meteorological Wind Tunnel	6
2.	Arrangement of model in test section	9
3.	Plan view of SNUPPS model	11
4.	Elevation views of SNUPPS model	12
5.	Plan view of STRIDE model	14
6.	Elevation view of STRIDE model	15
7.	Typical anemometer calibration curve	18
8.	Flame ionization detector calibration curves for methane and ethylene	20
9.	Development of mean velocity profile along centerline of wind tunnel; U_∞ = 6 m/s	22
10.	Lateral profiles of mean velocity; U_∞ = 6 m/s	23
11.	Development of longitudinal turbulence intensity along centerline of wind tunnel; U_∞ = 6 m/s	24
12.	Development of mean velocity profile in log-law form along centerline of wind tunnel; U_∞ = 6 m/s	27
13.	Normalized mean velocity as a function of non-dimensional height compared with the 1/6 power law curve; x_m = 11.5 m	28
14.	Concentration profiles for a ground level point source; (a) lateral, (b) vertical (linear plot)	29
15.	Concentration profiles for a ground level point source; (a) lateral, (b) vertical (semi-log plot)	30

NUMBER	TITLE	PAGE
16.	Concentration profiles for a point source with a 50 meter release height; (a) lateral, (b) vertical	31
17.	Concentration profiles for a point source with a 100 m release height; (a) lateral, (b) vertical	32
18.	Dispersion coefficients compared with those of Pasquill-Gifford (Turner, 1970); (a) lateral, (b) vertical....	34
19.	Dispersion coefficients compared with those of Pasquill-Gifford D stability class normalized by the roughness length; (a) lateral, (b) vertical	35
20.	Dispersion coefficients compared with stability classes from the Julich study (Vogt, 1977) for 50 m source height; (a) lateral, (b) vertical.....	36
21.	Dispersion coefficients compared with stability classes from the Julich study (Vogt, 1977) for 100 m source height; (a) lateral, (b) vertical	37
22.	Dispersion coefficients for ground level and 100 m source heights compared with stability classes from the St. Louis study (McElroy, 1969).....	39
23.	Instaneous photograph of the STACK model with a 50 m release height	41
24.	Photographs of releases from the SNUPPS model; (a) ABS for 0° wind angle, (b) DEV for 90° wind angle	42
25.	Photographs of releases from the STRIDE model RIV for 0° incident wind angle; (a) instantaneous, (b) 10-sec continuous exposure	43
26.	Pasquill-Gifford vertical stability classes plotted with the NRC building wake correction (NRC Reg. Guide 1.111, 1977) and the "unrestricted" wake correction for the SNUPPS power plant	45
27.	Pasquill-Gifford lateral stability classes plotted with the NRC building wake correction (NRC Reg. Guide 1.111, 1977) and the "unrestricted" wake correction for the SNUPPS power plant.....	46
28.	Building wake functions for the SNUPPS model; (a) lateral, (b) vertical.....	47

NUMBER	TITLE	PAGE
29.	Building wake functions for the STRIDE model; (a) lateral, (b) vertical.....	49
30.	Wake functions for all SNUPPS release cases plotted by regression parameter; (a) lateral with estimated projected building areas, (b) vertical.....	53
31.	Wake functions for all STRIDE release cases plotted by regression parameter; (a) lateral, (b) vertical.....	54
32.	Wake functions for the SNUPPS model normalized by the maximum building width or height; (a) lateral, (b) vertical..	55
33.	A comparison of SNUPPS and STRIDE wake functions: normalized by the projected building area; (a) lateral, (b) vertical and normalized by the square root of the projected building area; (c) lateral, (d) vertical.....	56

TABLES

Number		Page
1.	SNUPPS release data	13
2.	STRIDE release data	16
3.	Parameter comparison of simulated and atmospheric flows	26
4.	Continuity checks on effluent releases from the STACK model	38
5.	Regression parameters for a plot of $\log_{10}$ (σ) versus $\log_{10}$ (distance downwind) for the SNUPPS model	50
6.	Regression parameters for a plot of $\log_{10}$ (σ) versus $\log_{10}$ (distance downwind) for the STRIDE model	51

SYMBOLS

A -- projected area of building normal to wind direction

C -- concentration, parts tracer per part air by volume

D -- inside diameter of stack

d -- displacement height

h -- building height

h_s -- stack height

k -- von Kàrmàn constant (0.4)

L -- width of building or group of buildings

P -- power law index

Q -- emission rate

Re -- Reynolds number

S -- lot area

s -- silhouette area

U -- mean wind speed

U_∞ -- maximum mean wind speed (free stream)

$U_\star$ -- friction velocity

W -- effluent speed

x -- downwind distance

y -- lateral distance perpendicular to wind direction

z -- height above ground surface

z_o -- aerodynamic roughness length

δ -- boundary layer depth

ν -- kinematic viscosity of air

Σ -- corrected standard deviation

σ_y -- standard deviation of lateral plume spread

σ_z -- standard deviation of vertical plume spread

SUBSCRIPTS

$(\ )_m$ -- model scale

$(\ )_f$ -- full scale

SECTION 1

INTRODUCTION

An important energy source for electrical power generation is the light-water-cooled reactor (LWR) nuclear power facility. The two most common types of LWR facilities are the boiling water reactor (BWR) and the pressurized water reactor (PWR). Relative to health, safety, environmental impact, and building design, an important consideration for a LWR facility is the assessment of any nuclear, as well as conventional, pollutants that might be released. Environmental impact calculations of the atmospheric transport of radiopollutants are usually based on the Gaussian equation for turbulent diffusion of passive contaminants in the atmosphere. Consequently, diffusion experiments include the determination of the diffusion parameters (Gaussian standard deviations), as well as other relevant parameters, for different structural, meteorological, topographical, and release conditions. A variety of diffusion parameter data sets, derived by various methods and applicable to various situations, are used.

A recent international meeting (Hoffman et al, 1978) brought into focus several areas where further research is needed such as the effect of the wake downwind of a power plant on the diffusion parameters (σ_y and σ_z) and the validation of the variation of diffusion parameters. There are numerous mathematical models available that can be used to assess the radiological consequences of routine and accidental releases of radionuclides from nuclear power facilities. Information extracted from such models can be inherently uncertain, since the transport and the dose can only be approximated. To examine the usefulness of a model as an assessment tool, a determination of the extent of this uncertainty is required.

Until recently these uncertainties had not aroused much interest in the scientific community, because of the conservative nature of the model predictions. This conservative nature was due to the adoption of conservative assumptions about exposure pathways, parameter values, and receptor characteristics. In the past, this approach was acceptable because model predictions were only a small fraction of the applicable standards, and the probability of individuals receiving doses in excess of the model predictions was remote.

Increasingly restrictive radiological protection standards have revived interest in developing more accurate models. Efforts are now underway to reduce excessive conservatism in the models and thus improve their accuracy (Hoffman et al, 1978). To bring prediction models into a more realistic realm, model parameters and basic assumptions must be reevaluated to determine

the predictive capabilities of the various models used in radiological assessments.

Government, as well as industry, strongly desires to establish "standard nuclear power plant designs" especially for BWR and PWR facilities. At present, there are approximately four architect-engineering (A/E) companies in the United States involved in the standardization of LWR nuclear power facilities. Three A/E companies are working with the standard design of PWR systems and one with the standard design of the BWR system. The goal is to reduce licensing time, engineering effort, construction schedules, and cost as well as better availability of money. Standardization would help to reduce the chances of design errors, since construction changes would vary little from one plant to the next. Also, fewer site-specific variables would considerably reduce A/E work load. The reduction in site-specific variables also has definite advantages when estimating atmospheric transport and dispersion of gaseous effluent releases from light-water-cooled nuclear power facilities.

The purpose of this study was to determine, through wind tunnel experiments, the diffusion parameters needed to update dose calculations relative to the dispersion of radiopollutants near standardized plants. In the wind tunnel, effluent concentrations were measured in the vicinity of the model facilities. Dispersion parameters were measured for three incident wind angles with two and four release points for the PWR and BWR, respectively. Ethylene was released from model plants as a tracer, and a flame ionization detector (FID) was used to obtain quantitative measurements of dispersion patterns.

The investigation of building-wake effects associated with standard design nuclear power plants will aid in assessing the near-building and downwind hazard associated with releases of radioactive effluents. The overall study provided a much needed interface between the point of effluent release and the usually assumed Gaussian plume. In the present study, horizontal and vertical dispersion coefficients, σ_y and σ_z, were determined experimentally in the wind tunnel for a simulated boundary layer and were found to be comparable to those of Julich (Vogt, 1977) and St. Louis (McElroy, 1969); they compared less well with Pasquill-Gifford (Turner, 1970) because of the much larger roughness length in the present experiments.

This wind tunnel study was limited to the simulation of neutral flow conditions and does not address the current problem of low wind speed, inversion conditions where wind meander becomes a significant dispersion mechanism. In principle, concentration patterns observed under different wind directions could be superposed to obtain longer term average concentrations thus accounting for wind meander effects, but additional study is required to determine the feasibility of such.

SECTION 2

CONCLUSIONS

1. An atmospheric flow over a suburban environment was simulated. The model roughness length was calculated to be 3.1 mm in the wind tunnel, which corresponds to a prototype roughness length of approximately 1.0 m for a 1:300 scale suburban area. Vertical profiles of velocity and turbulence intensity were representative of those found in atmospheric flows over suburban areas. A boundary layer with the above specifications may be used for a variety of transport and diffusion studies over short to moderate downwind distances.

2. The agreement of dispersion parameters measured in the wind tunnel with standard Pasquill-Gifford curves was poor; this may be expected because the Pasquill-Gifford curves were derived for surfaces with roughness length of approximately 10 cm. When data from the present study and that of Pasquill-Gifford were normalized by roughness length, the agreement was good. Dispersion parameters measured in the present study also agreed well with the respective parameters measured in suburban area field studies. Data from full scale measurements in the Julich and St. Louis experiments tended to confirm that scale modeling of a suburban atmospheric boundary layer with properly scaled diffusion parameters had been achieved. It can be concluded that diffusion in the atmosphere was simulated in the wind tunnel.

3. Wake effects for the two standardized nuclear power plants were described by plume standard deviations. For the power plant with the greater ratio of length to width, a change in incident wind angle altered the plume spread by as much as a factor of two, and in one case, altered the rate of growth of the plume. In all cases lateral plume spread was related directly to the silhouette area of the buildings. For both power plants, the measured plume spread was not noticeably different for different stacks. The indistinguishability of stack releases was ascribed to the high turbulence and rapid mixing associated with structures of complex shape.

4. In all cases, the lateral and vertical standard deviations calculated with the Nuclear Regulatory Commission (NRC) building wake correction formula were smaller than those measured in the laboratory. This is a trend that indicates the NRC building wake correction calculations consistently yield over-estimates of maximum concentrations and doses.

5. A graphical method to calculate the lateral plume spread in the wake of a building or building complex of known projected area was developed. This technique promises to be of practical use in calculating building wake characteristics.

6. Attempts were made to relate the calculated building wake functions to physical aspects of the individual power plants. The silhouette or projected area and, to a lesser degree, the square root of the silhouette or projected area proved to be normalizing factors for lateral plume spread. No such simplification was found for vertical plume spread.

SECTION 3

EXPERIMENTAL EQUIPMENT AND PROCEDURES

THE METEOROLCGICAL WIND TUNNEL

The study was undertaken in the EPA Meteorological Wind Tunnel (MWT) (Figure 1). It is an ultra-low speed, open-return wind tunnel with a test section 2.1 m in height, 3.7 m in width, and 18.3 m in length. To remove room air turbulence and produce a uniform velocity profile, exterior air passes through a honeycomb, a series of four screens, and a 2.8 to 1 contraction before entering the test section. After flowing through the test section, the air flow passes through an acoustic silencer, a rectangular to round transition section, the fan, a diffuser, and another acoustic silencer before being exhausted back into the room. The ceiling height of the test section can be adjusted to compensate for the blockage effects of a model placed in the wind tunnel. An instrument carriage mounted on rails within the test section can position a probe anywhere within a 17 m x 3 m x 1.5 m volume with accuracy of ± 1 mm. Laboratory data are sampled, processed, and stored by a Digital Equipment Corporation (DEC) PDP 11/40 minicomputer. Real time capabilities and disk or magnetic tape storage provide instant feedback of data being taken as well as easy access for later analysis. A detailed description of the EPA Meteorological Wind Tunnel may be found in Snyder (1979).

DESIGN OF THE EXPERIMENT

The study consisted of qualitative and quantitative experimentation. The primary objective was to determine building wake effects by measuring effluent concentration fields associated with two standard design nuclear power plants for three incident wind angles. The examination of building wakes and the parameter comparisons were quantitative. Flow visualization by photographing an oil fog effluent provided the qualitative part of the study, which corroborated the quantitative concentration data. Experimentally determined diffusion coefficients for an undisturbed flow were compared with the atmospheric values of Turner (1970), Vogt (1977), and McElroy (1969) which are most often applied.

Three models were used in the present study: an isolated stack, a standard design PWR nuclear power plant, and a standard design BWR nuclear power plant. The isolated stack model (STACK) was used to determine the dispersion characteristics of the simulated atmospheric boundary layer. The two standard design nuclear power plants were examined to determine the building wake effects associated with the dispersion of effluent releases. The

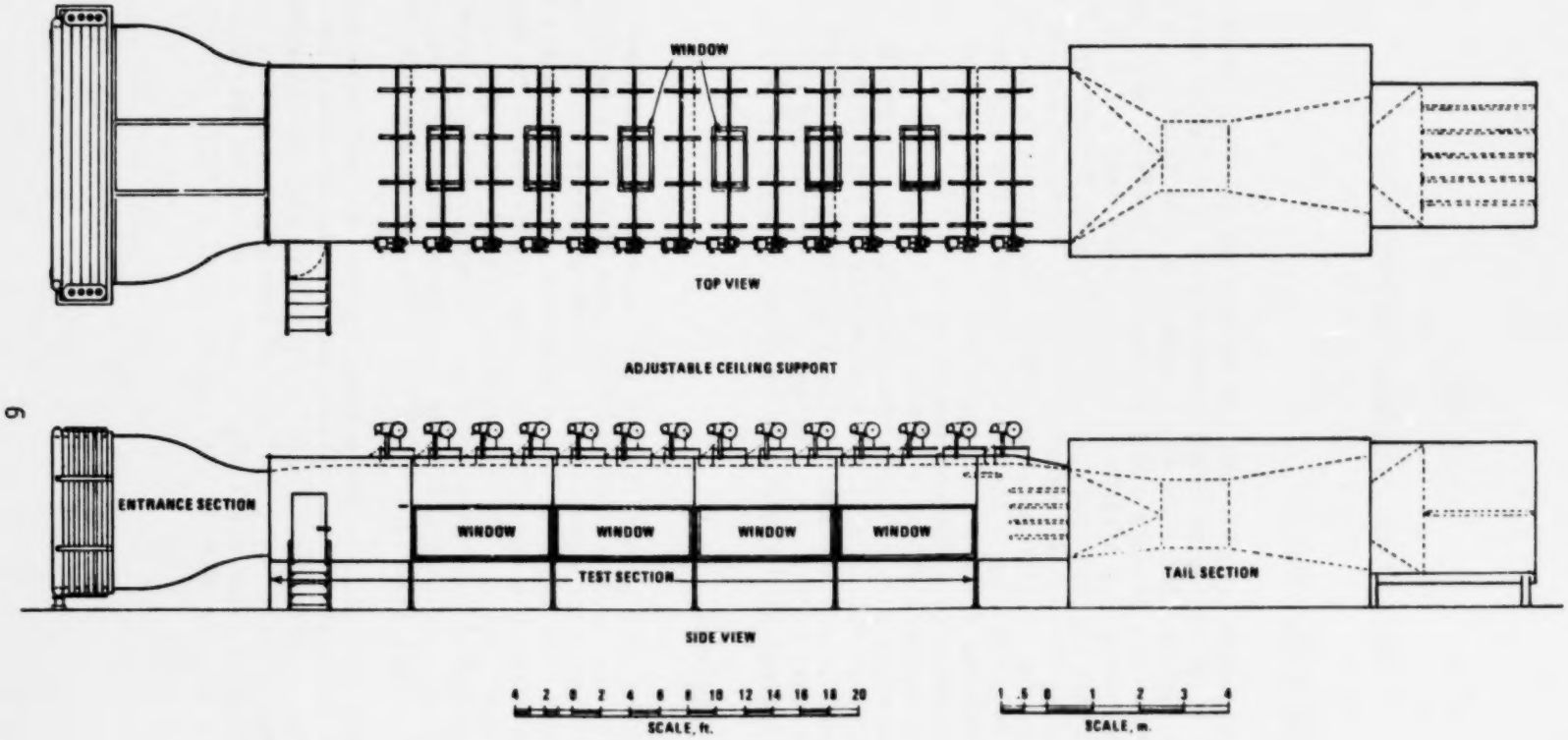

Figure 1. Overall plan and elevation of the EPA Meteorological Wind Tunnel.

standardized nuclear power plants used were the Standard Nuclear Power Plant System (SNUPPS), a PWR power plant vended by the Bechtel Corporation, Gaithersburg, Maryland and the Standard Reactor Island Design (STRIDE), a BWR power plant vended by C.F. Braun and Company, San Jose, California. These two plants were selected because STRIDE is the only standardized BWR power plant and SNUPPS is quite similar in shape to the other PWR standard designs.

The study focused on the near-field effluent concentrations in the range from the immediate vicinity to approximately 20 building heights downwind of the standardized plants. The models were constructed of acrylic plastic, except for the domes which were made of wood and the stacks which were brass tubes. A model to prototype scale ratio of 1:300 was followed.

Similarity Criteria

For the behavior of the flow in the MWT to simulate that in the atmosphere, it was necessary to match certain nondimensional parameters (Snyder, 1972; 1981). For the present study the parameters of significance were:

$$\frac{L}{h}\ ,\ \frac{D}{h}\ ,\ \frac{h_s}{h}\ ,\ \frac{\delta}{h}\ ,\ \frac{W}{U}\ ,\ \frac{Uh}{\nu}\ ,\ \text{and}\ \frac{WD}{\nu}\ .$$

The building-complex width-to-height ratio, L/h; the stack diameter to building height ratio, D/h; the stack height to building height ratio, h_s/h; and the boundary layer thickness to building height ratio, δ/h, satisfied the similarity criteria because the models were scaled-down versions of the full-scale plants. The effluent exit speed to wind speed ratio, W/U, determines the plume rise for a nonbuoyant plume. This ratio was strictly modeled on information provided by utilities and architect-engineers.

The final two similarity criteria considered were the building-complex Reynolds number, $Re_b = Uh/\nu$, and the effluent Reynolds number, $Re_e = WD/\nu$. For exact similarity, the building-complex Reynolds number of the model must equal that of the prototype. Matching of Reynolds numbers was not possible because of the scale of the models that was used. Fortunately, this criterion is not necessary, because at sufficiently large Reynolds numbers, the flow patterns become independent of Reynolds number (Snyder, 1972). In the present study, building Reynolds numbers ranged from approximately 60,000 to 80,000 with a freestream wind speed of 6 m/s. These values are well above critical Reynolds numbers with sharp-edged buildings, and of the same order of magnitude as critical values associated with more streamlined buildings (Halitsky, 1977).

It was imperative that the study simulate atmospheric conditions as accurately as possible. In neutral atmospheric flows, all major flow systems are turbulent, and viscous forces are relatively unimportant. Thus, except very near the surface, the flow is considered Reynolds-number independent. If the surface is roughened so that the irregularities are larger than the thickness of the viscous sublayer, an aerodynamically rough surface is created (Sutton, 1949). The domes and cylinders associated with the two model power

plants were covered with sand, attached by epoxy cement. The sand caused protrusions on the surface approximately 1.0 mm high. SNUPPS, the power plant with a hemispherical dome, was designed with structural supports that acted as trips to aid turbulence. STRIDE had a dome of large curvature and a sharp edge at the top of the cylindrical reactor buildings. The design features and the roughened surfaces helped insure an aerodynamically rough surface so that the flow was Reynolds-number independent (Slade, 1968).

The criterion of turbulent flow associated with the effluent Reynolds number, WD/ν, was satisfied. A trip consisting of an internally serrated washer was placed in the stack, 10 stack diameters upstream from the exit, to insure a fully turbulent flow upon release (Liu and Lin, 1976). This technique enabled the plume behavior to be independent of effluent Reynolds number (Snyder and Lawson, 1976). Effluent Reynolds numbers ranged from 1250 to 2050 without the trips.

Wind Tunnel Arrangement

The simulated flow should possess properties characteristic of the appropriate atmospheric flow. To observe plume dispersion or building wake effects in a boundary layer in the wind tunnel, the undisturbed flow must be essentially two-dimensional and change very little in the streamwise direction. Subsequent to the initial development, the simulated flow becomes a typical boundary layer flow and it is appropriate to compare the properties of the developed flow with those of naturally grown boundary layer flows. In the present study, a simulated neutrally stable "suburban" flow was compared to its full-scale counterpart. The choice of the term "suburban" was based on roughness length exclusively. Nuclear power plants are usually placed in areas of low population density. These areas are normally arable or forested having intermediate surface roughness characterized by the term "suburban". No consideration was given to the pros or cons of placing a nuclear plant in the outlying part of a city or town. The term "suburban" in the present study is used to indicate intermediate roughness length and should not be associated with population density.

The experimental technique used to simulate a neutrally stable suburban atmospheric boundary layer consisted of a straight barrier 235 mm in height placed at the entrance to the MWT test section. The floor of the test section was covered with three-dimensional roughness elements measuring 14 mm x 14 mm x 150 mm on 150 mm centers (see Figure 2). This boundary layer development scheme evolved from that described by Counihan (1969).

Positions in the wind tunnel are represented by a rectangular cartesian coordinate system where x, y, and z are defined as the longitudinal, lateral, and vertical directions, respectively, and U, V, and W are the velocities in the x, y, and z directions, respectively. The origin for all undisturbed flow measurements (i.e. without a model present) was located at the beginning of the roughness elements immediately behind the barrier ($x = 0$), at the centerline ($y = 0$), and on the floor ($z = 0$). For measurements associated with the models, the lateral and vertical locations of the origin were un-

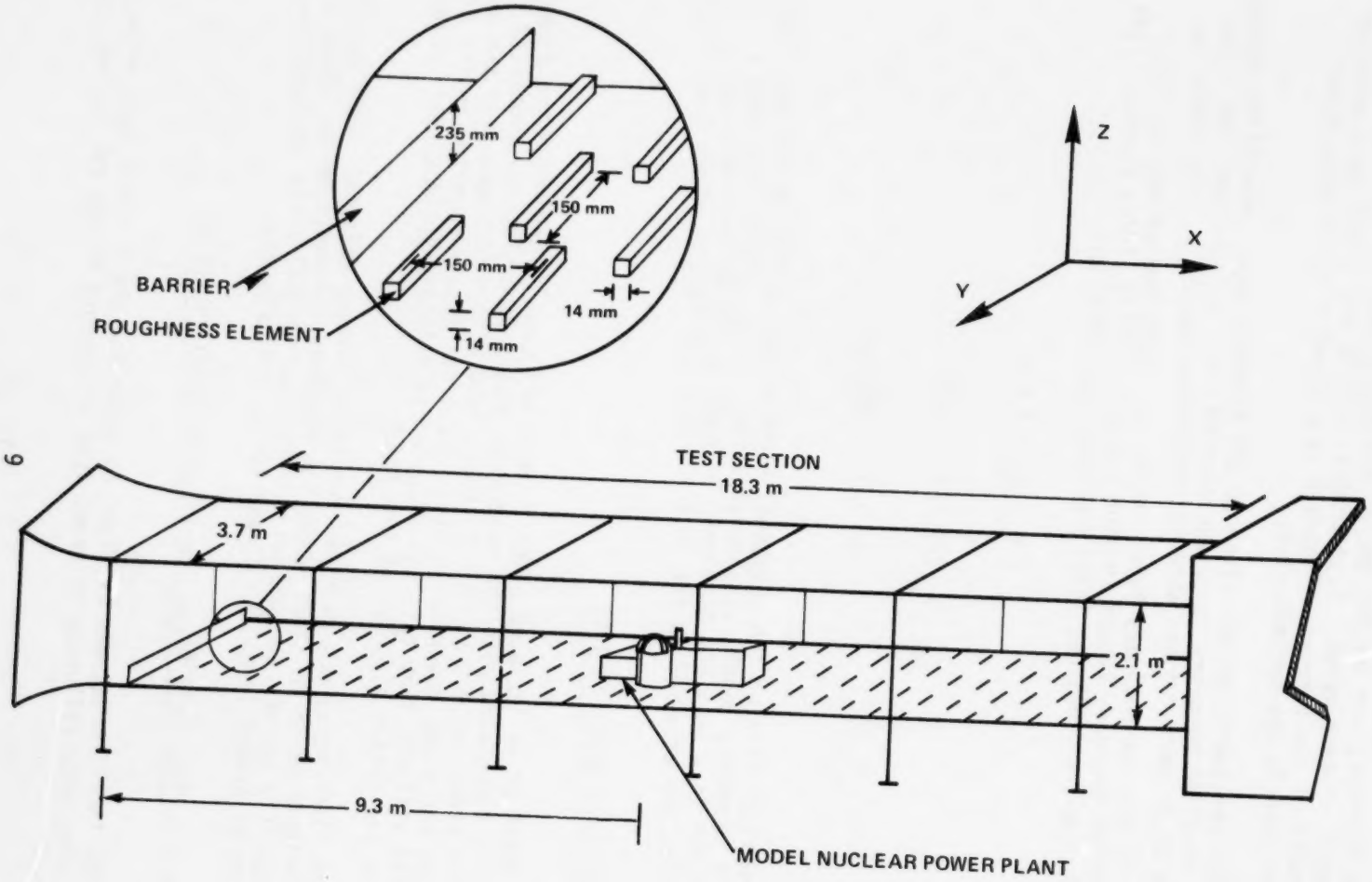

Figure 2. Arrangement of model in test section.

changed, but the location of x = 0 was altered for convenience. For the STACK model, x = 0 was at the point of release from the stack, 9.3 m downwind of the barrier, and for the SNUPPS and STRIDE models, x = 0 was the most downwind point of each model. Both models, SNUPPS and STRIDE were centered 9.3 m downwind of the barrier. Figure 2 is a drawing of the wind tunnel arrangement used in the present study.

Careful consideration was given to the boundary layer generation scheme because a specific boundary layer was desired, i.e. a "suburban" one. The parameters of primary concern were the roughness length, z_o, the power law exponent, P, and the boundary layer depth, δ. Suggested values for full-scale suburban boundary layers (Wilson and Netterville, 1978; Kaufman, 1977; Castro, Jackson, and Robins, 1975; and Counihan, 1975) are:

$$1.0 \leq z_o \leq 1.5 \text{ m}$$

$$1/6 \leq P \leq 1/4$$

$$150 \leq \delta \leq 600 \text{ m}.$$

The appropriate size of the roughness elements was estimated (Lettau, 1969) and floor roughness panels were constructed. These panels consisted of approximately 3,000 14 x 14 x 150 mm blocks of wood on 150 mm centers glued to sheets of masonite and attached to the 18.3 x 3.7 m test section floor (see Figure 2).

Isolated Stack Model (STACK)

A model of an isolated stack release was used to determine the dispersion parameters associated with the neutrally stable suburban flow simulated in the MWT. The stack was a 0.56 cm i.d. brass tube with a 90° bend near the exit directing the plume downwind to avoid any cross-stream momentum in the effluent. The effluent flow rate was adjusted to maintain an isokinetic release based on the inside diameter of the stack.

The STACK model was examined for three release heights. Wind tunnel release heights of 15 mm (just above the roughness elements on the floor of the wind tunnel), 166 mm, and 333 mm corresponded to full scale isolated stack releases of ground level, 50 m, and 100 m, respectively.

Standard Nuclear Unit Power Plant System Model (SNUPPS)

The SNUPPS model was utilized to determine the building wake effects associated with effluents released from a standard design PWR nuclear power

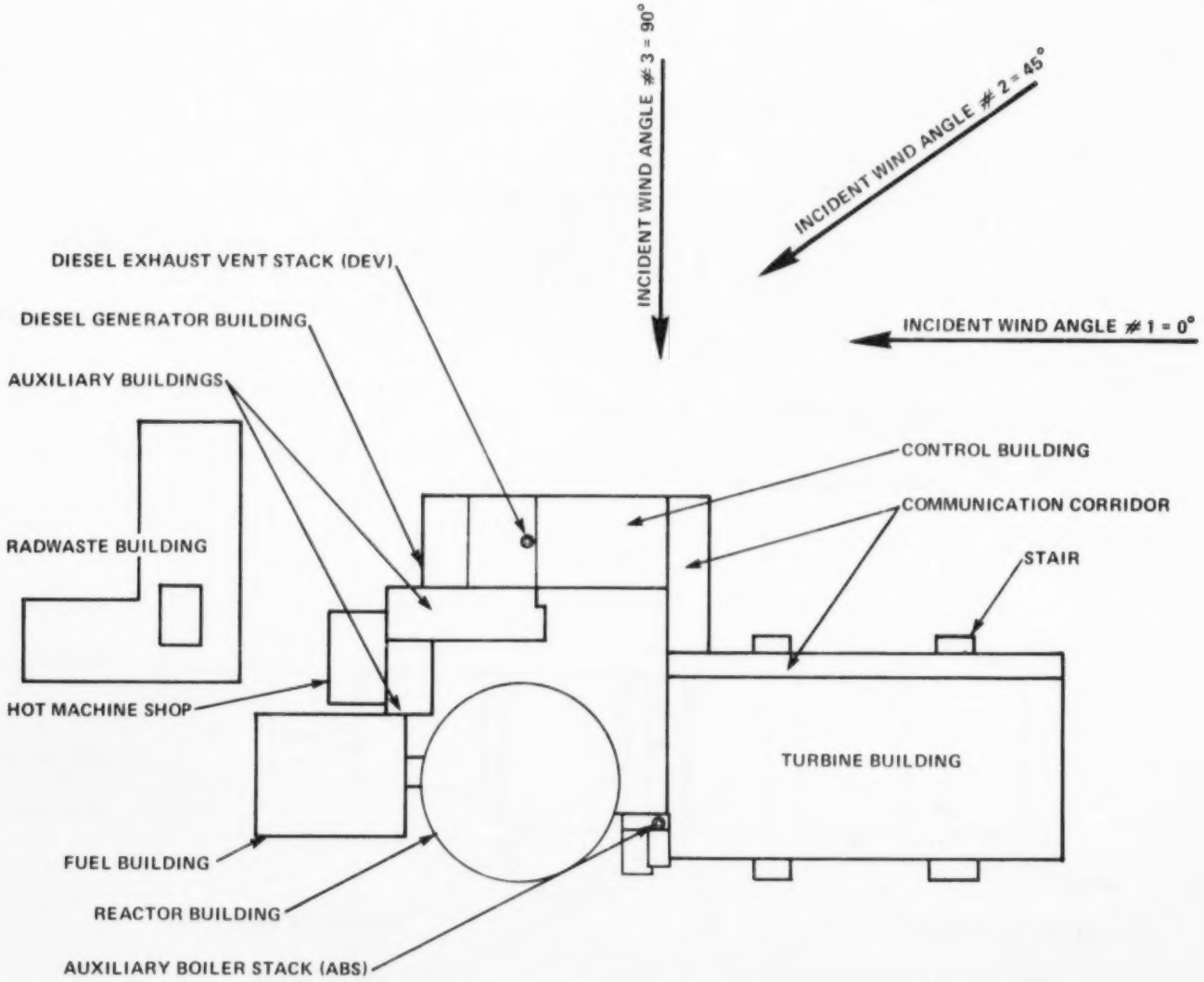

Figure 3. Plan view of SNUPPS model.

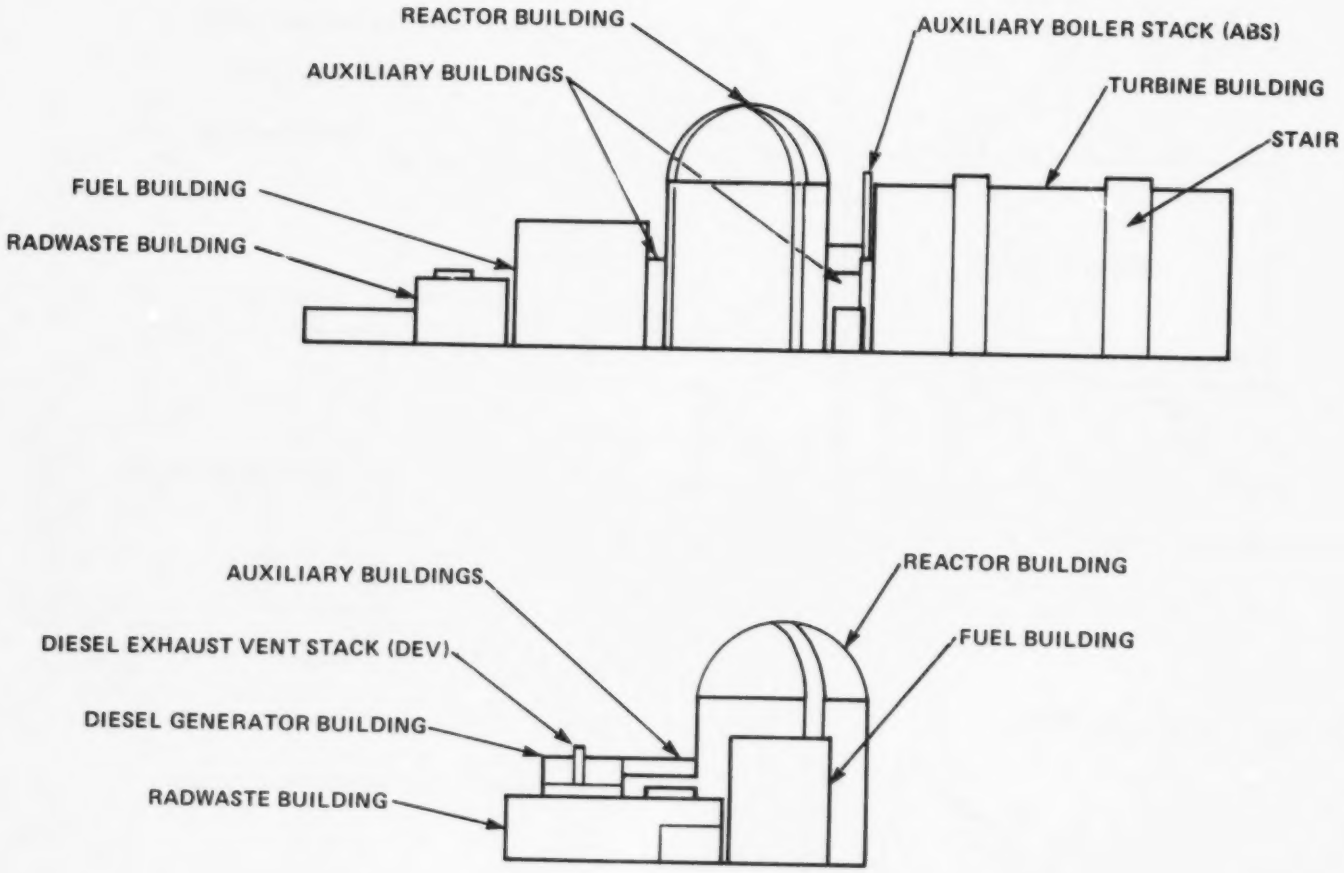

Figure 4. Elevation views of SNUPPS model.

TABLE 1. SNUPPS RELEASE DATA

Parameter	Full scale	Model scale
ABS[a] inside diameter	2.1 m (7 ft.)	0.71 cm (9/32 in.)
ABS stack height	47.7 m	15.9 cm
ABS release rate	10.8 m^3/s (23,000 CFM)	6,300 cc/min
DEV[b] inside diameter	0.6 m (2 stacks, each 2 ft.)	0.39 cm (5/32 in. 1 stack)
DEV stack height	29.7 m	9.9 cm
DEV release rate	2.36 m^3/s (5,000 CFM)	2,900 cc/min

(a) ABS = auxiliary boiler stack

(b) DEV = diesel exhaust vent

plant. The model had maximum overall dimensions of 86.2 x 35.4 x 21.3 cm. Figures 3 and 4 are top and elevation views of the SNUPPS model. The stack diameters and exit velocities of the effluent were modeled to simulate those of an operating, full scale plant. Releases were neutrally buoyant. Table 1 is a summary of the SNUPPS release data.

The dispersion was examined for effluent releases at three different incident wind directions. Since most dispersion corrections for wake effects are associated with building dimensions (height, width, or cross-sectional area), the incident wind directions were selected to maximize and minimize the dimensions associated with the building-complex. Figure 3 depicts incident wind angles 1 (0°), 2 (45°), and 3 (90°) which correspond to the minimum, the maximum, and an intermediate cross-sectional area, respectively. Measurements were taken for effluent releases from each stack for all wind directions.

Standard Reactor Island Design Model (STRIDE)

The STRIDE model was used to determine the building wake effects associated with effluents released from a standard design BWR nuclear power plant. The model had maximum overall dimensions of 61.0 x 70.5 x 17.4 cm. Figures 5 and 6 are top and elevation views of the STRIDE model. The stack diameters and exit velocities of the effluent were modeled to simulate that of an operating full scale plant. Releases were neutrally buoyant. Table 2 is a summary of the STRIDE release data.

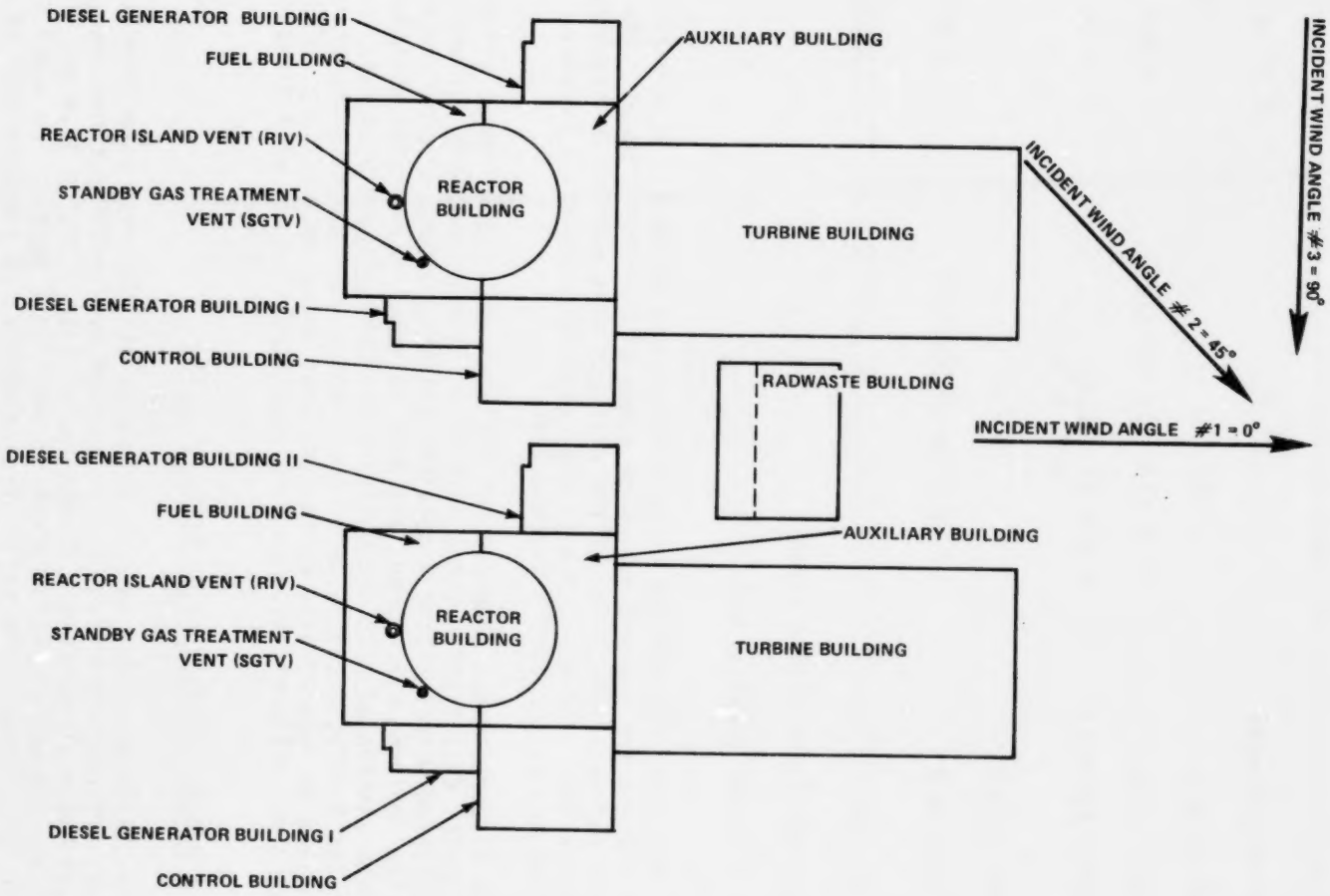

Figure 5. Plan view of STRIDE model.

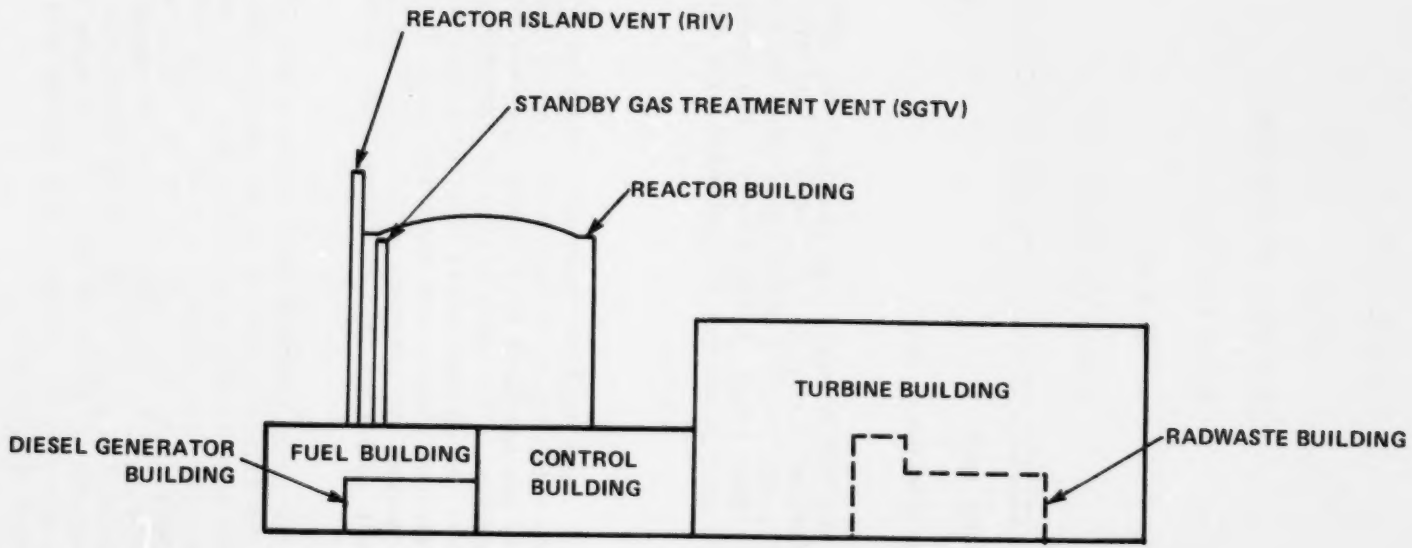

Figure 6. Elevation view of STRIDE model.

TABLE 2. STRIDE RELEASE DATA

Parameter	Full scale	Model scale
RIV[a] inside diameter	1.5 m (5 ft.)	0.51 cm (7/32 in.)
RIV stack height	58.2 m	19.4 cm
RIV release rate	10.8 m^3/s (23,000 CFM)	7,300 cc/min
SGTV[b] inside diameter	0.5 m (18 in.)	0.16 cm (1/16 in.)
SGTV stack height	46.8 m	15.6 cm
SGTV release rate	2.36 m^3/s (5,000 CFM)	1,700 cc/min

(a) RIV = reactor island vent

(b) SGTV = standby gas treatment vent

Dispersion from the STRIDE model was examined for effluent releases at three different incident wind angles. Figure 5 illustrates incident wind angles 1 (0°), 2 (45°), and 3 (90°) which correspond to intermediate, maximum, and minimum cross-sectional areas, respectively. Measurements were taken for effluent releases from each stack for all incident wind directions.

FLOW VISUALIZATION

An extensive flow visualization study was conducted on the STACK, SNUPPS, and STRIDE models before taking any concentration measurements. Smoke for the qualitative flow study was produced by a Kenney Engineering model 1075SG paraffin oil fog generator. The smoke generator operates by aspirating paraffin oil onto a heating element which creates a fine oil fog. Flow rates associated with the various stacks were monitored with Meriam Laminar Flow Elements which were checked for accuracy with a bubble meter and stopwatch. The smoke generator was connected in-line between the laminar flow element and the stack.

Photographs of the smoke patterns were taken with a 35 mm camera using ASA 400 black and white film and ASA 160 color transparency film. Side views and overhead views for each model, wind angle, and stack were taken. Photographs taken at an ambient wind speed of 6 m per second and effluent emission rates prescribed by model scaling proved to be of little value. The smoke plumes were not dense enough to produce adequate photographs. Each plume was visually evaluated under the above release conditions, the wind speed and emission rate were reduced by a factor of 3, and reevaluated visually. No noticeable plume characteristics changed. All photographs were subsequently taken under the reduced flow speeds.

VELOCITY MEASUREMENTS

Velocity and turbulence measurements were made with Thermo-Systems Incorporated (TSI) constant temperature anemometers. Two types of anemometer probes were used. Most measurements were taken with a TSI model 1210-20 hot-film probe, which provided one-dimensional information on velocities and turbulence intensities. Corroborative measurements were made with a TSI model 1241-20 cross, hot-film endflow probe. The cross film probe provided the capability of two-dimensional velocity and turbulence intensity measurements. The anemometer output signals were digitized at a rate of 250 samples per second, linearized, and processed on the PDP-11/40 minicomputer. A mean freestream windspeed of 6 m/s was used for all quantitative measurements. Reasonably repeatable results (approximately ± 1% mean velocity) were achieved using a sampling time of 60 seconds.

Anemometer calibration curves were determined in the freestream flow. The hot-film probes were calibrated by placing them adjacent to a pitot tube for comparison. Calibration sampling times and rates were 20 seconds and 50 samples per second, respectively. Six to eight calibration points were established over the velocity range 1.5 to 8.5 m/s. The best fit to a variation of King's Law, $E^2 = A + B\,U^{\alpha}$, was determined where E was the output voltage of the anemometer, U was the mean velocity, and A, B, and α were constants determined in the calibration. The best fit was associated with the α that minimized the sum of the squared errors. A typical calibration curve is shown in Figure 7.

Velocity profiles were acquired by the computer sampling the anemometer output. A table showing digitized voltage versus velocity was generated according to the best fit values of A, B, and α acquired from the calibration. During the sampling period, a reference table was prepared for linearization. At the completion of each sampling period, the mean velocities, the root-mean-square (rms) velocities and the turbulence intensities were computed. Due to the sensitivity of the hot-film probes to ambient temperature, the room temperature was monitored continuously. If a temperature change of 0.5° C was detected, the new temperature was entered into the computer, which calculated a new reference table according to

$$E^2 = (A + BU^{\alpha})\,[(T_f - T_{new})/(T_f - T_{cal})]$$

where T_f is the film temperature, T_{new} is the new room temperature, and T_{cal} is the room temperature at which the probe was calibrated. The new look-up table was used until updated again.

CONCENTRATION MEASUREMENTS

Concentration profiles were obtained using a Beckman model 400 Hydrocarbon Analyzer (flame ionization detector, FID) in the continuous operating mode. Samples were collected through 1.6 mm teflon tubing with a brass

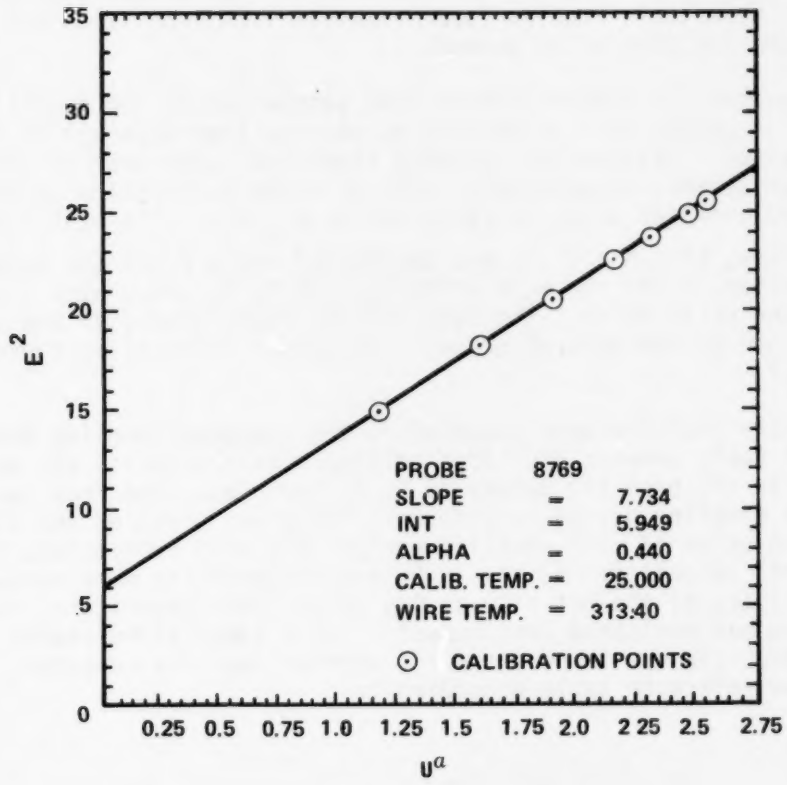

Figure 7. Typical anemometer calibration curve.

tube as a sampling probe. The brass probe was mounted on the instrument carriage and incremented through the hydrocarbon plume such that the intake gas was analyzed by the FID for its hydrocarbon content at each location.

The instruments were calibrated each day before they were used. Zero air, with less than 1 ppm total hydrocarbon, was used to set the "zero" or minimum detection level of the FID. A 1% methane gas was used to set the "span" or maximum level of detection. Ethylene (99% pure) was chosen as the tracer gas because of its neutrally buoyant properties in air. Ethylene and air have molecular weights of approximately the same value, 28.0 and 28.9, respectively. Since the difference in the number of carbon atoms in the molecules of the tracer gas (C_2H_4) and the calibration gas (CH_4) resulted in a different response for the FID, calibration was run to determine appropriate "response factors" for each gas. The response factors were used to normalize the data relative to the calibration standard, thus response factors were determined to be 1.0 and 1.6 for methane and ethylene, respectively. The response of the FID was linear for both gases in the measurement region. The calibration curves for the two gases are shown in Figure 8. The "zero" and "span" were checked after each series of calibration profiles to ensure that the electronics had not drifted.

The output of the FID was processed by the PDP-11/40 minicomputer. The background level of hydrocarbons in the room air would increase during the sequence of concentration measurements because the tunnel air recirculated through the room. To correct for the increase in background hydrocarbons, background concentration measurements were taken during the experiment, at least at the beginning and end of a profile, and on occasion more frequently. A computer program bracketed data between adjacent background measurements, subtracting the background hydrocarbon concentration from the sample concentration by assuming a linear change in background with time between measurements. The response time of the FID was approximately 0.5 seconds, too large to obtain useful statistics on concentration fluctuations.

SIMULATION OF A SUBURBAN ATMOSPHERIC BOUNDARY LAYER

The simulation of an undisturbed suburban atmospheric boundary layer was necessary to make relevant comparisons between differing building wake characteristics. Accurate measurements of the flow and dispersion associated with this undisturbed boundary layer were required. Considerable effort was expended developing the boundary layer. Several wind tunnel arrangements were used and analyzed before an appropriate boundary layer was developed. Different wind tunnel arrangements were produced by using different combinations of roughness elements, barrier heights, barrier shapes, and vortex generators. Criteria used in selecting the proper wind tunnel arrangement were (1) an adequate fit to the power law and log-law equations which were used to describe the boundary layer, (2) an adequate boundary layer depth, (3) a large enough z_o, and (4) laterally homogeneous velocity profiles. The wind tunnel arrangement selected for use in the present study is shown in Figure 2.

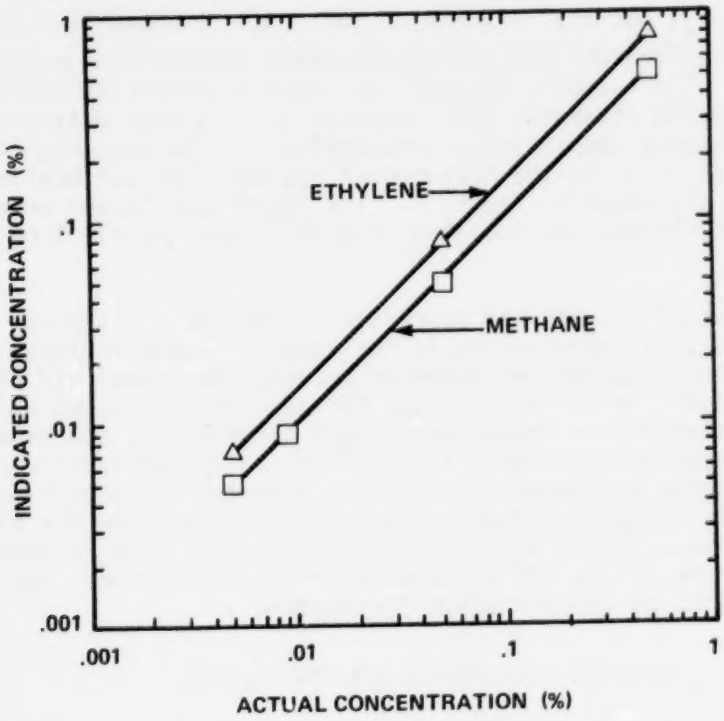

Figure 8. Flame ionization detector calibration curves.

SECTION 4

RESULTS AND DISCUSSION

THE SUBURBAN BOUNDARY LAYER

Velocity Measurements

To examine the development of the boundary layer, vertical velocity profiles were taken at various longitudinal positions on the centerline of the tunnel. Profiles were acquired at 4.0 m, 8.0 m, 11.5 m, and 15.0 m downwind of the barrier and are displayed in Figure 9. The boundary layer was not completely developed at x_m = 4.0 m, as shown by the flatness of the profile at heights between 150 mm and 400 mm. This abnormality is barely discernible at x_m = 8 m, and is absent farther downstream. For practical purposes, it may be concluded that the boundary layer was fully developed at x_m = 9.0 m.

Lateral profiles were taken at several downwind distances to examine lateral homogeneity. In all cases where the vortex generators were used adjacent to the barrier, there were nonuniformities. Figure 10 shows examples of lateral velocity profiles with and without the vortex generators. The final wind tunnel arrangement did not use vortex generators.

Figure 11 shows the development of turbulence intensity as a function of downstream distance. The turbulence intensity decreases at the top of the fully developed boundary layer to approximately 10% of that near the surface. The development of the turbulence intensity also indicates fully developed flow at $x_m \geq 9.0$ m.

A sequence of semi-log plots of wind speed versus height is presented in Figure 12. The straight-line requirement of a fully developed flow is emphasized dramatically in the figure. Obviously, the flow had not fully developed by x_m = 4.0 m, but had adequately developed by $x_m > 8.0$ m. The boundary layer depth, δ, was approximately 1250 mm. An extrapolation of each curve indicates values of 3.0 to 3.3 mm for the roughness length, z_o, in the fully developed flow. A least squares fit to the lower 20% of the data at x_m = 11.5 m determined z_o to be 3.1 mm or approximately 1.0 m in the atmosphere.

These experiments led to positioning the models at the upwind edge of the "fully developed" boundary layer. The boundary layer was developing throughout the length of the MWT. However, it could be considered fully developed

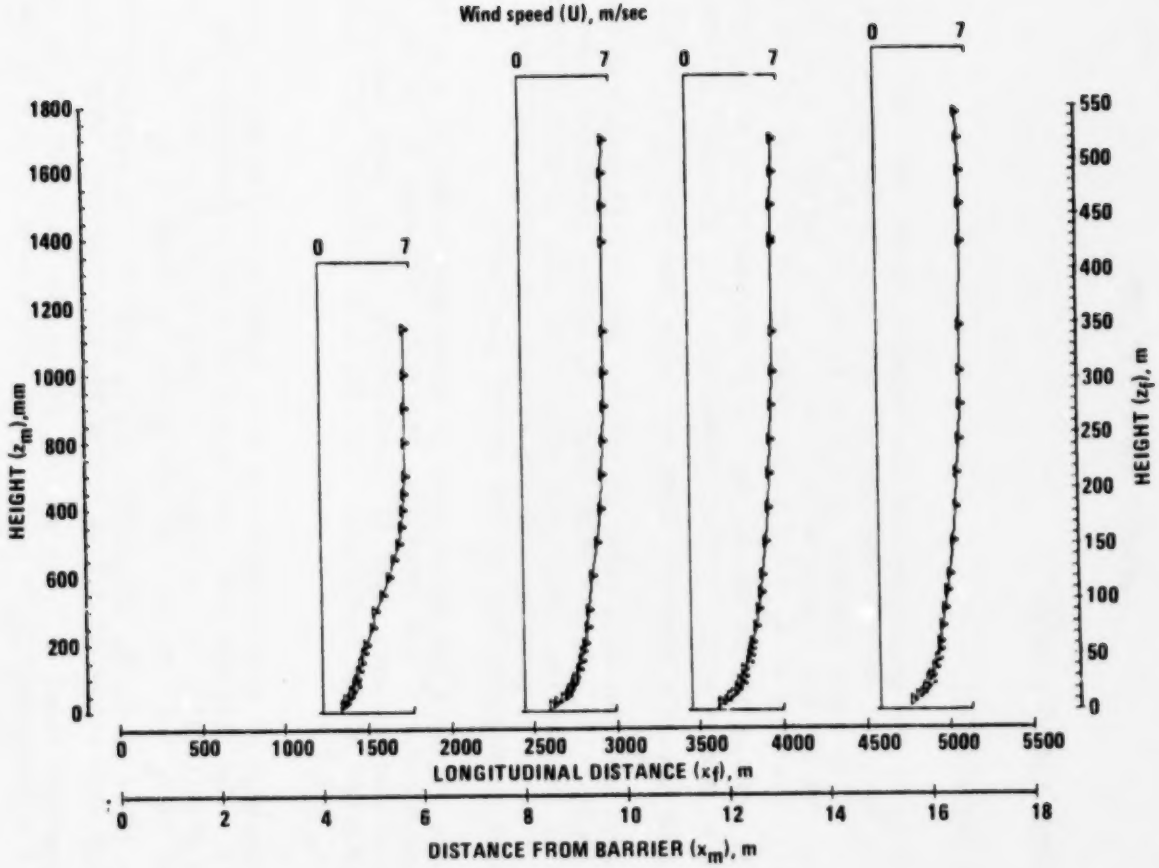

Figure 9. Development of mean velocity profile along centerline of wind tunnel; U_∞ = 6 m/s.

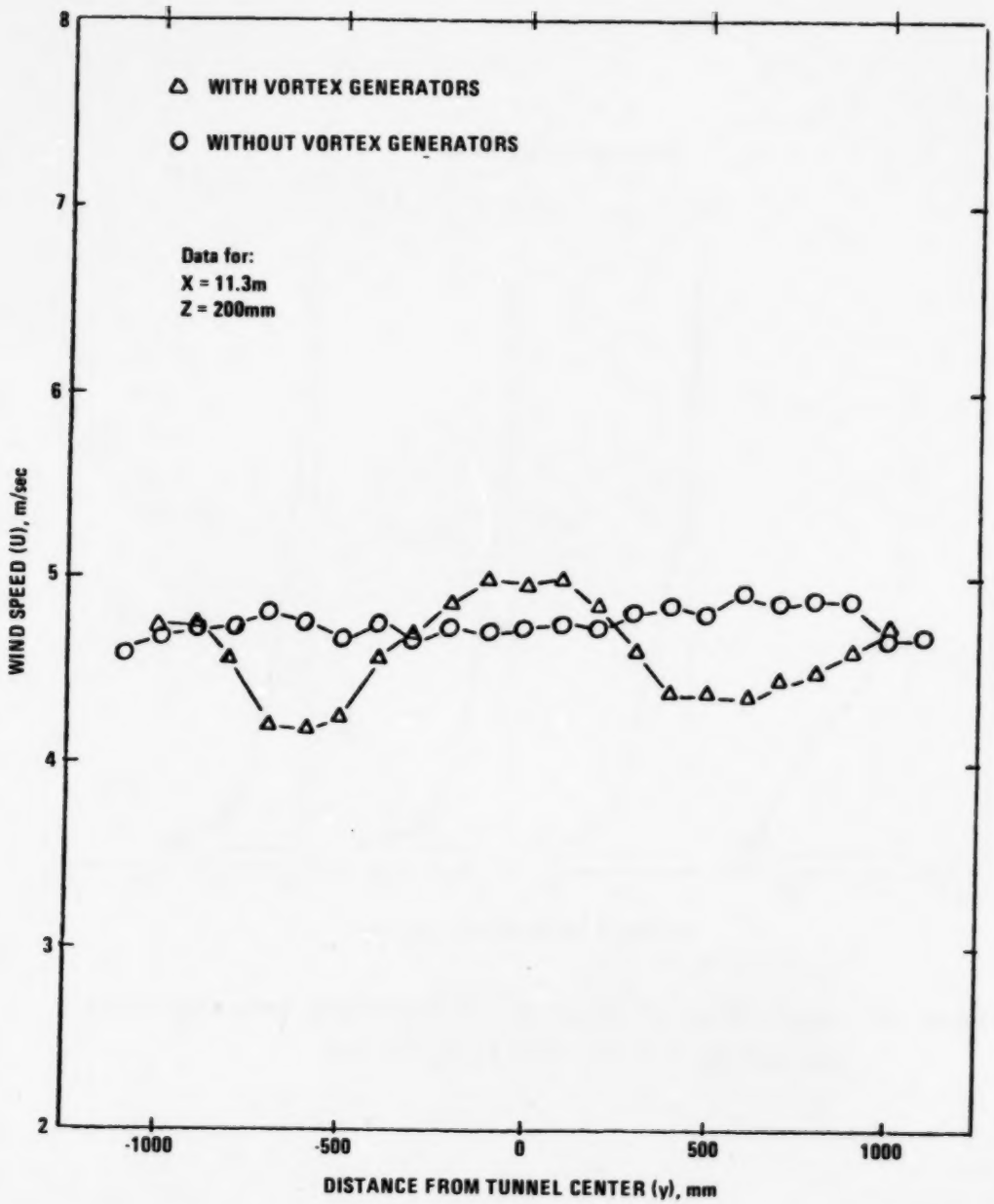

Figure 10. Lateral profiles of mean velocity; U_∞ = 6 m/s.

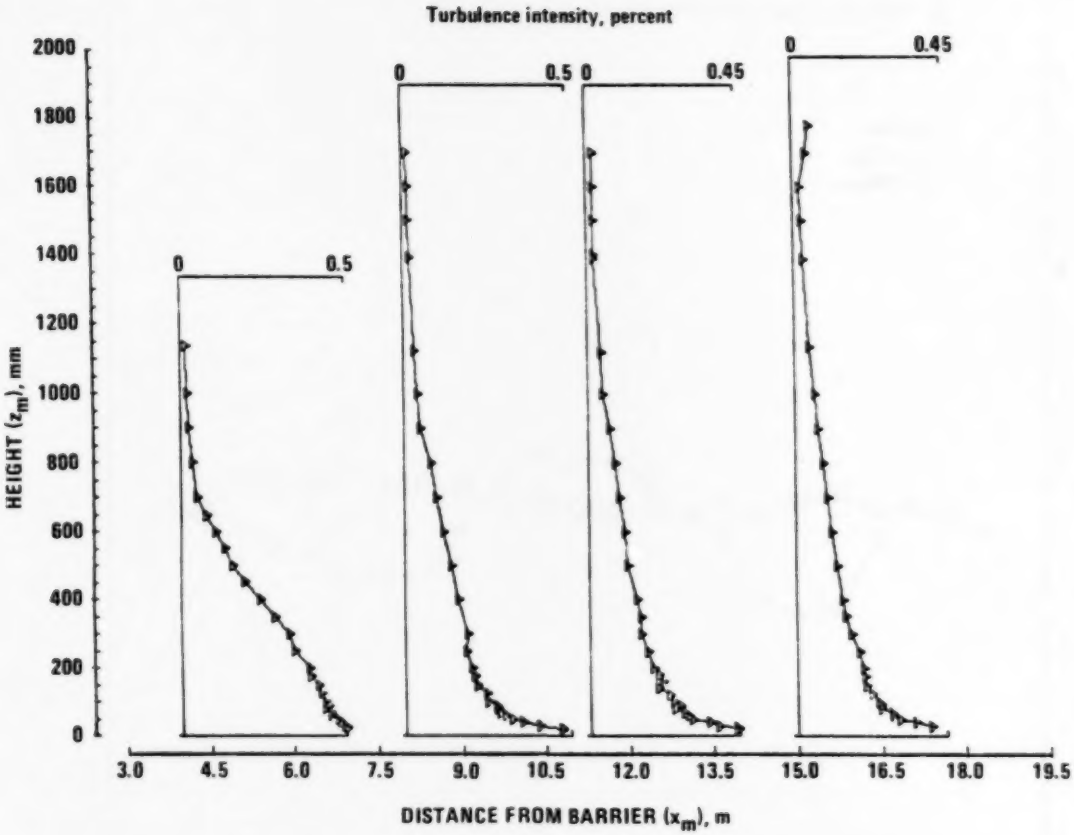

Figure 11. Development of longitudinal turbulence intensity along centerline of wind tunnel; U_∞ = 6 m/s.

at approximately x_m = 9 m since development thereafter was minimal (see Figures 9, 11, and 12). The models were placed 9.3 m from the barrier, allowing 9.0 m of test section available for downstream measurements.

A comparison of the parameters determined in the present study with those of simulated and atmospheric flows obtained by other investigators is shown in Table 3. Agreement is good. The ratio U^*/U_∞ is slightly high. The ratio was determined from the slope of the semi-log plot of a mean velocity profile (Figure 12). Direct measurements with cross-film anemometry tend to be lower (Castro, 1980). Figure 13 is a vertical velocity profile at x_m = 11.5 m. The data fit well to a 1/6 power law relationship.

Dispersion Characteristics of the Boundary Layer

Dispersion of the simulated suburban boundary layer was examined by measuring downwind concentrations of ethylene released from a point source (the STACK model). Vertical and lateral concentration profiles were acquired at downstream distances of 0.25 m, 0.5 m, 0.86 m, 1.77 m, and 5.0 m, which corresponds to full scale distances of 75 m, 150 m, 250 m, 530 m, and 1500 m, respectively.

For each of the three stack heights, sets of concentration profiles were plotted. The figures were plotted as normalized concentration, CU_∞/Q, versus a length, where C is the concentration in parts of hydrocarbon per part of air, U_∞ is the freestream velocity (6 m/s), and Q is the emission rate (m^3/sec). The length is plotted in full-scale units of meters, and refers to the height or lateral distance depending on the type of profile, vertical or lateral, respectively. The stack was located at the tunnel centerline (y = 0) and all vertical concentration profiles for the STACK model were taken at this location. Lateral profiles were taken at the height of the maximum concentration as determined from the vertical profiles.

Lateral and vertical concentration profiles for a ground level source are plotted in Figures 14 (a) and 14 (b) for the five downwind distances. Best fit Gaussian curves were successfully drawn through the data points. There is little resolution in the data taken at small values of CU_∞/Q for this type of plot. Figures 15 (a) and 15 (b) are the same data plotted on semi-log scales, which enhances the representation of the smaller values of CU_∞/Q and gives a better perspective of the Gaussian nature of the data, especially at farther downwind distances. All other data are plotted using the semi-log presentation Figures 16 and 17 are concentration profiles for point sources with release heights of 50 m and 100 m, respectively.

Lateral and vertical standard deviations (σ_y and σ_z, respectively) were calculated for the data presented in each profile. For the lateral profiles, the normal method of calculating the standard deviation was employed. For the vertical profiles, a computer program developed at the EPA Fluid Modeling Facility was used to calculate the standard deviation associated with a plume that is reflected from the ground.

TABLE 3. PARAMETER COMPARISON OF SIMULATED AND ATMOSPHERIC FLOWS

Source/Parameter	Flow Type	Model:Prototype Scale	Boundary Layer Depth, δ (m)	Roughness Length, z_o (m)	Power Law Index, P	Ratio of Friction Vel. to Freestream Vel., U_*/U_∞
Present Study	Simulated Suburban	1:300	1.25	1.0	0.17	0.07
Robins (1978)	Simulated Urban	1:300	2.0	1.3	0.22	0.063
Castro, Jackson, & Robins (1975)	Simulated Urban	1:300	2.0	1.3	0.2	0.065
Counihan (1975)	Full-scale Suburban	1:1	600	1.0-1.5	0.2	0.045-0.055

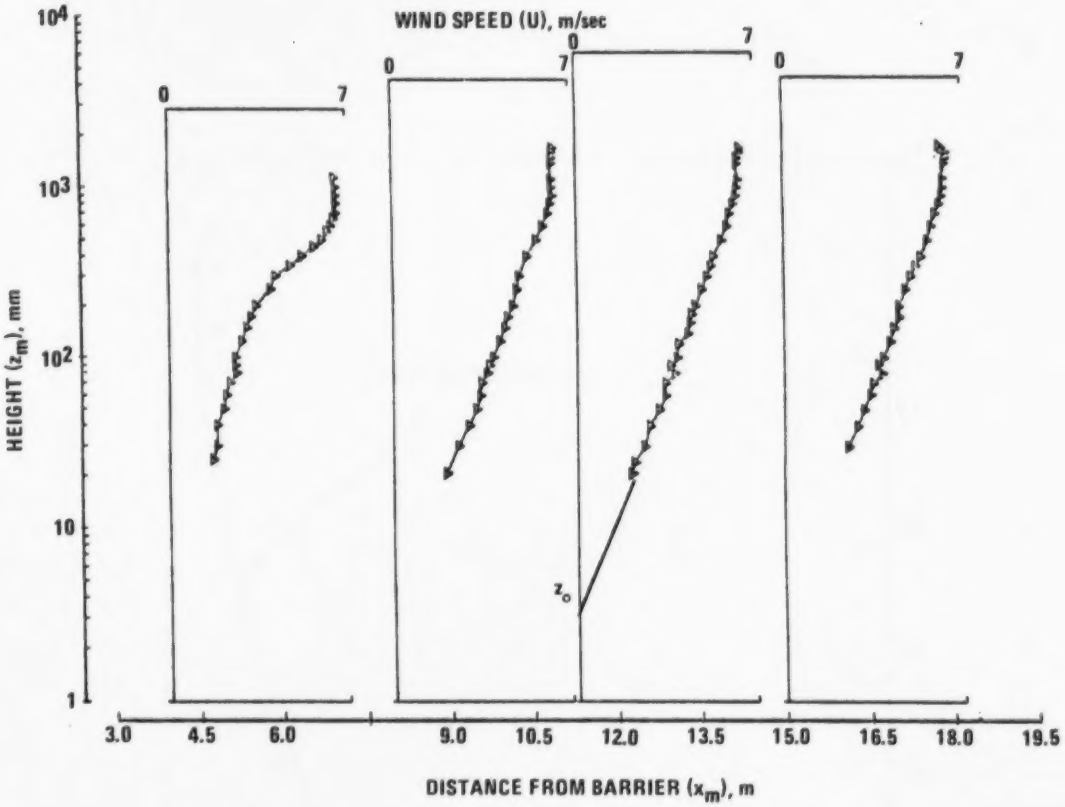

Figure 12. Development of mean velocity profile in log-law form along centerline of wind tunnel; U_∞ = 6 m/s.

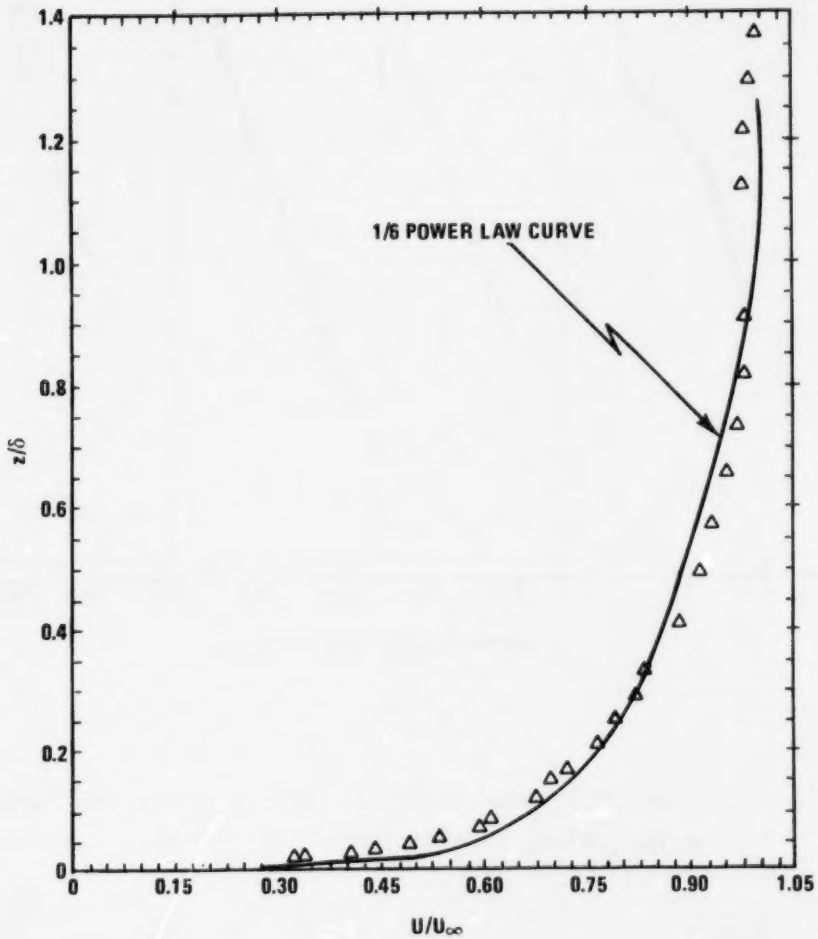

Figure 13. Normalized mean velocity as a function of non-dimensional height compared with the 1/6 power law curve; x_m = 11.5 m.

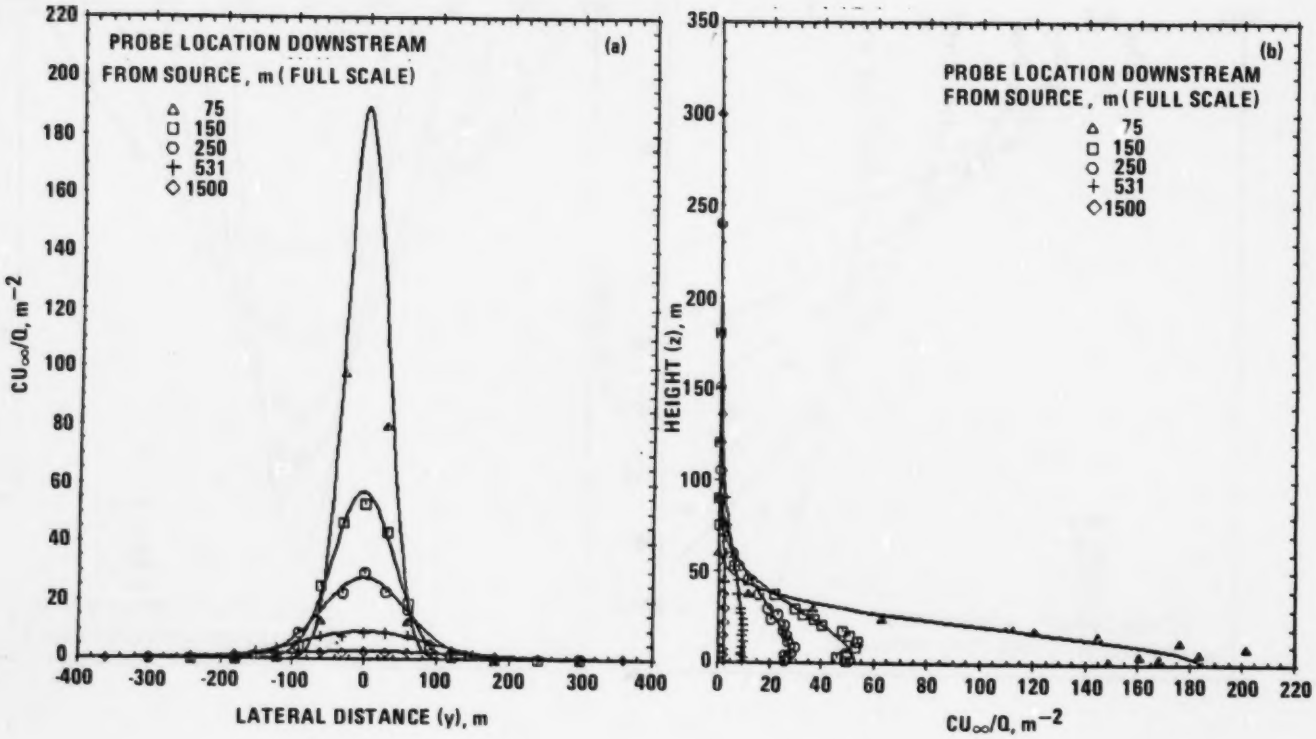

Figure 14. Concentration profiles for a ground level point source; (a) lateral, (b) vertical (linear plot).

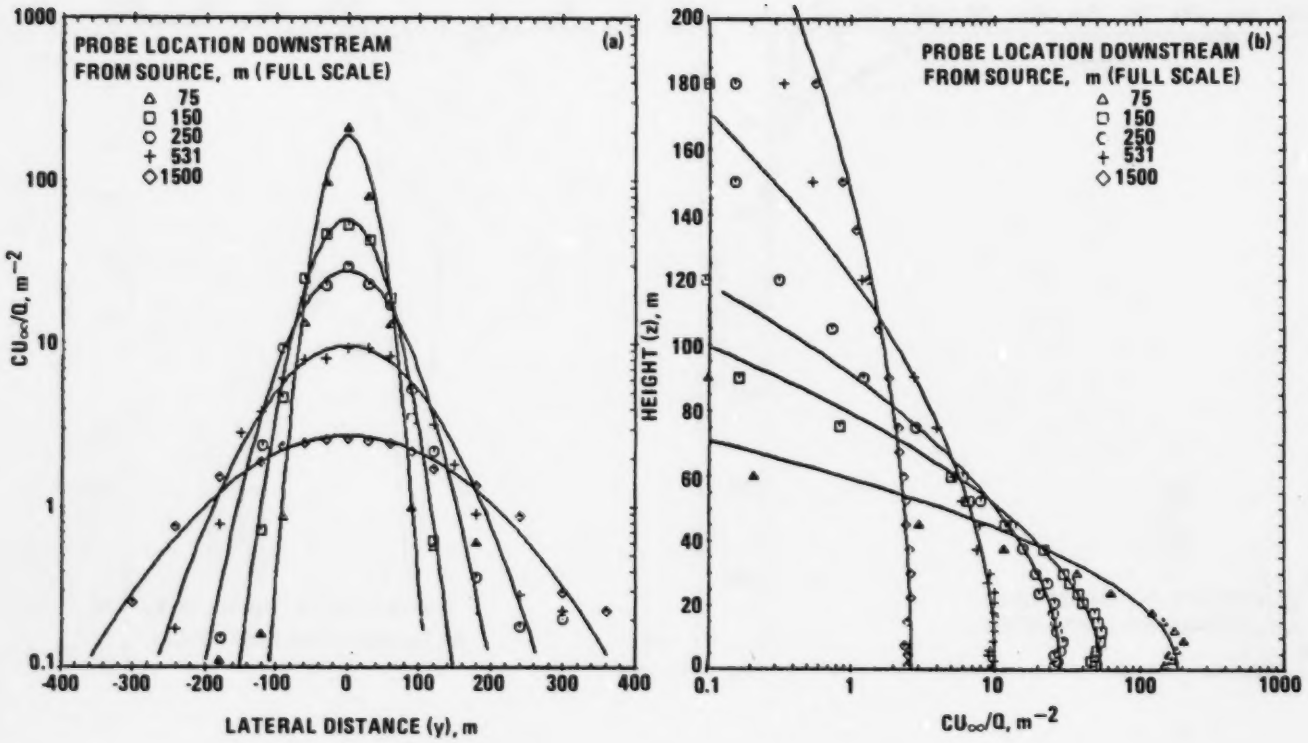

Figure 15. Concentration profiles for a ground level point source; (a) lateral, (b) vertical (semi-log plot).

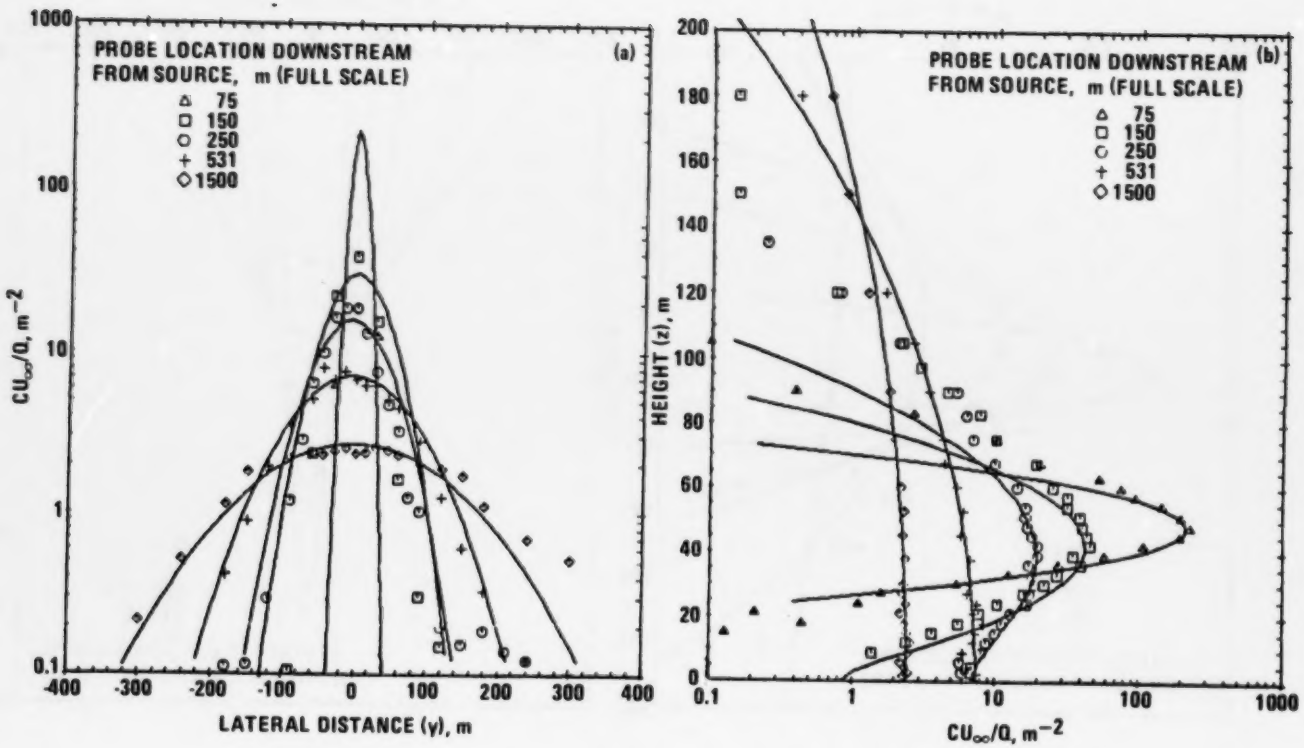

Figure 16. Concentration profiles for a point source with a 50 meter release height; (a) lateral, (b) vertical.

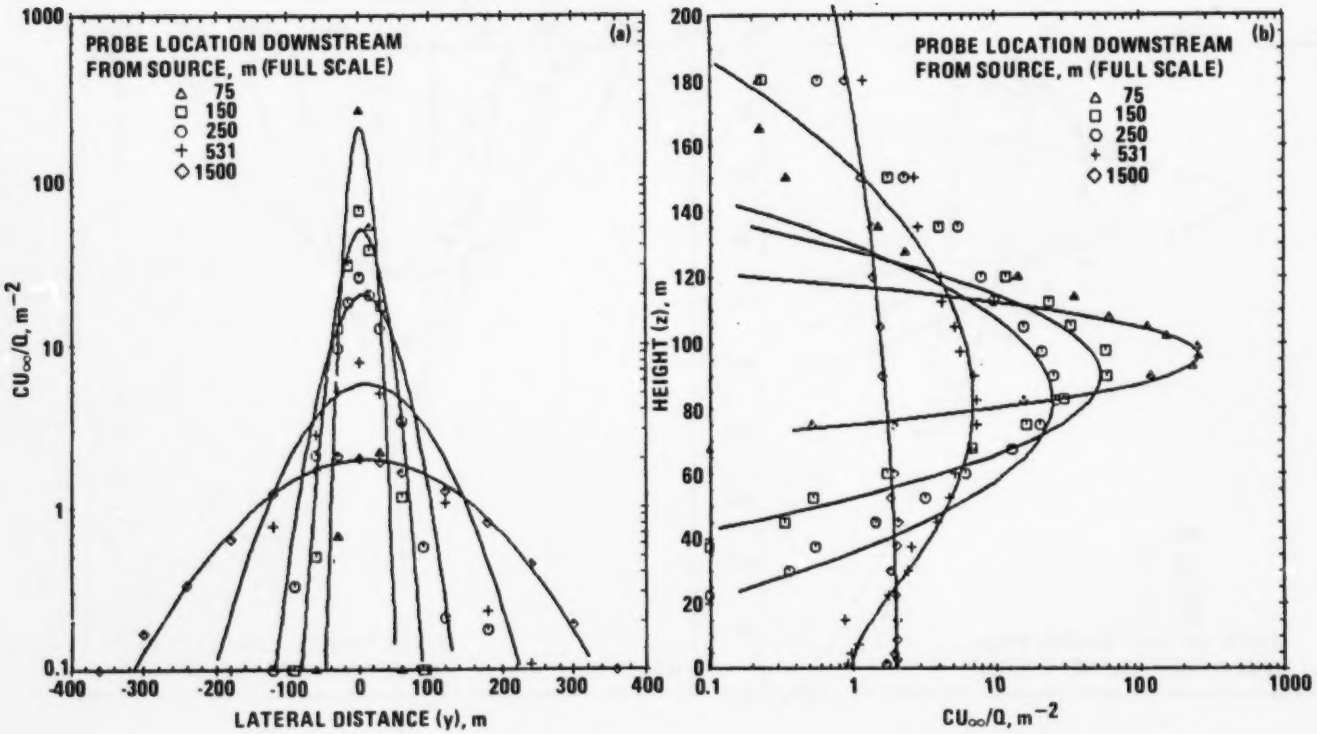

Figure 17. Concentration profiles for a point source with a 100 meter release height; (a) lateral, (b) vertical.

Mass continuity checks were made to insure that the amount of hydrocarbons released were being detected adequately in the associated lateral and vertical profiles. A computer program was used to perform the integration $\int\int CUdydz$, where C is the concentration and U is the velocity from a power law fit to a velocity profile at the same downstream location. The resultant value of $\int\int CUdydz$ was then divided by the emission rate, Q, to provide a reference value for the continuity check. For the ideal case, the Value of $\int\int CUdydz/Q$ would be equal to unity. Table 4 presents the continuity checks associated with each pair of concentration profiles for the STACK model. The data agree satisfactorily.

Comparisons of plume spreading rates are important to assess the accuracy with which the laboratory data can be applied to full scale situations. However, comparisons can be difficult considering the uncertainties that arise in predicting full scale spreading rates due to variations in local turbulence levels and stability. Figure 18 is a comparison of the lateral and vertical plume standard deviations obtained for a ground level source with those of Pasquill-Gifford (Turner, 1970). Near the source, the data indicate high instability; they tend toward more stable values farther downstream. This result agrees with other wind tunnel data for similar comparisons (Robins, 1978; Courtney, 1979). Comparisons of this type must be qualified. The present study represents flow over relatively rough terrain (z_o = 1.0 m). The Pasquill-Gifford curves are still applied very frequently in practice, but seldom do they accurately represent the terrain at a real site. In the present study, the disagreement with Pasquill-Gifford standard deviations was believed to be caused by the difference in roughness length. To compensate for the variation in terrain roughness, both sets of data were normalized by dividing by the roughness length, z_o. Figure 19 represents the improved agreement established by the normalization.

Since emission height is known to affect values obtained for the diffusion parameters, σ_y and σ_z, the present results are compared with those of the Julich experiments (Vogt, 1977). The comparison of the data for a 50 m source height is presented in Figure 20. The results agree remarkably well for neutral stability. Both sets of data correspond to equal roughness lengths as well as source height. Figure 21 is a plot of the same data sets for a 100 m source height. Again the agreement is quite close for neutral stability.

The data acquired in the St. Louis experiment (McElroy, 1969) were also plotted with that of the present study. This allowed a comparison of the present data with dispersion coefficients determined for an urban area. Figure 22 exhibits a very close relationship between the two sets of data. The ground level source data are very closely correlated with the St. Louis stability class for both the lateral and vertical plume spread. Both are low level releases over terrain of roughness length approximately 1.0 m.

The dispersion characteristics of the developed boundary layer are in very close agreement with the characteristics exhibited by atmospheric boundary layers over relatively rough surfaces. The poor agreement with the Pasquill-Gifford dispersion functions is believed to be due to the large difference in roughness lengths for the two experiments. Comparisons made between data acquired over terrain having similar roughness lengths (z_o approximately 1 m) proved to be quite good. All indications are that the desired suburban atmospheric boundary

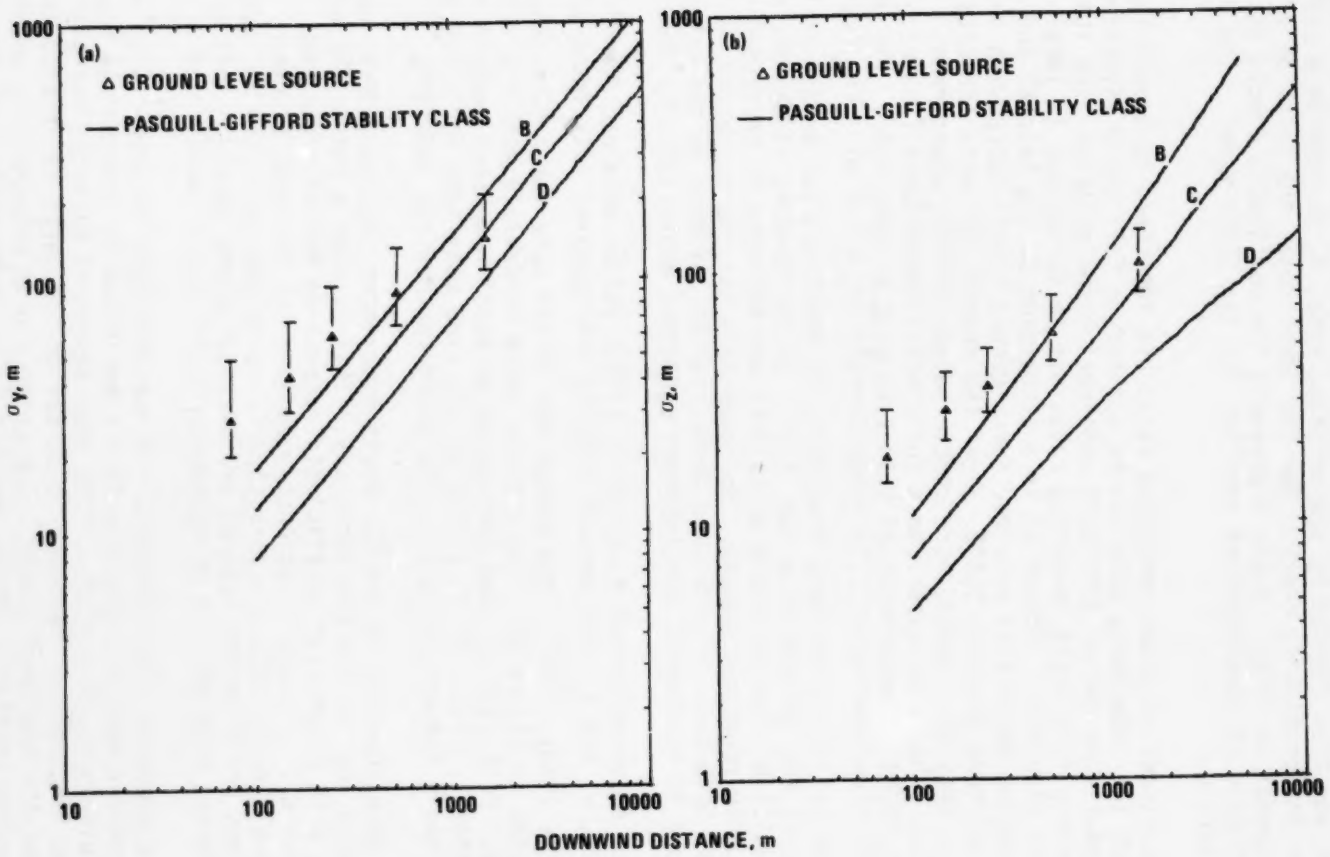

Figure 18. Dispersion coefficients compared with those of Pasquill-Gifford (Turner, 1970); (a) lateral, (b) vertical.

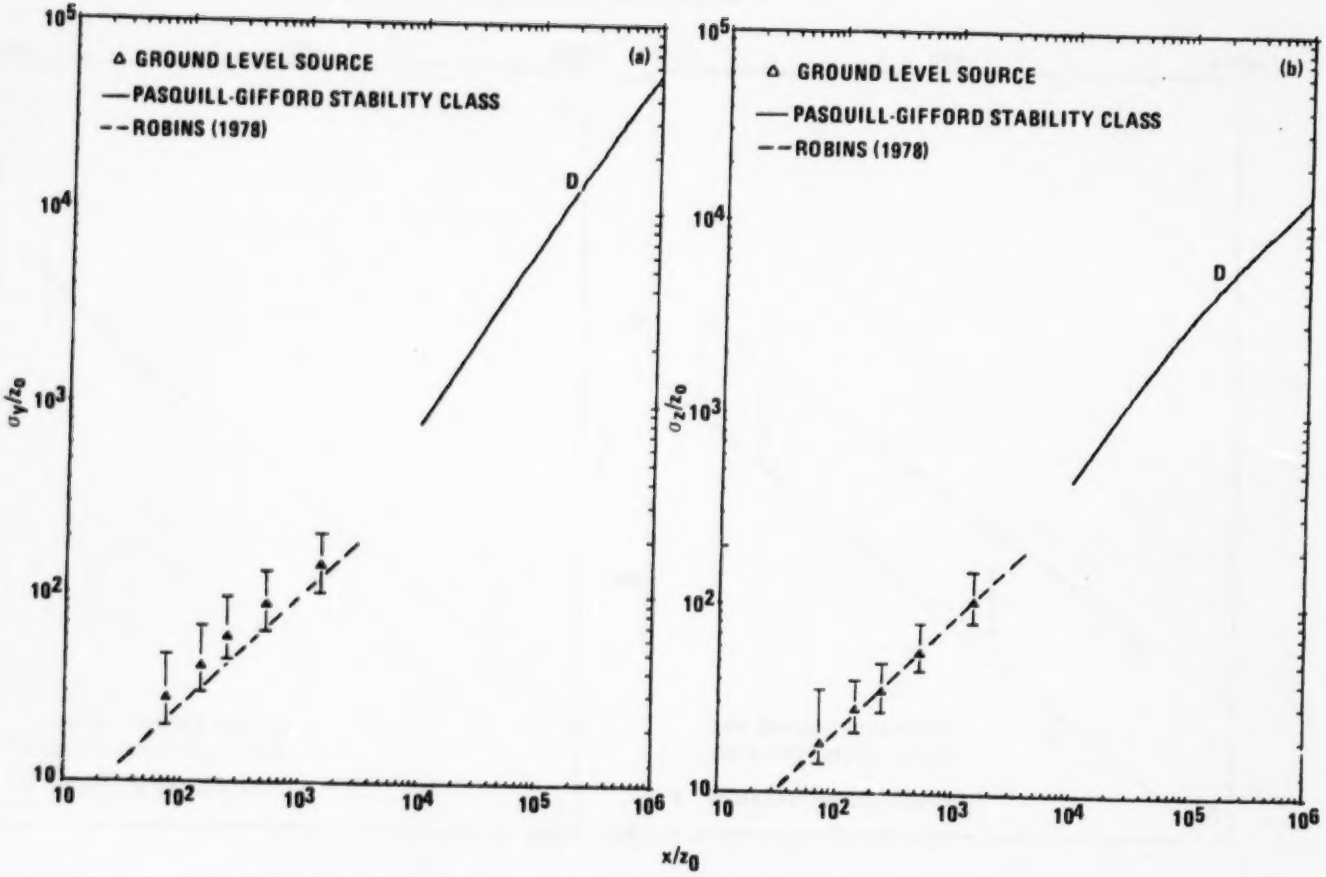

Figure 19. Dispersion coefficients compared with those of Pasquill-Gifford D stability class normalized by the roughness length; (a) lateral, (b) vertical.

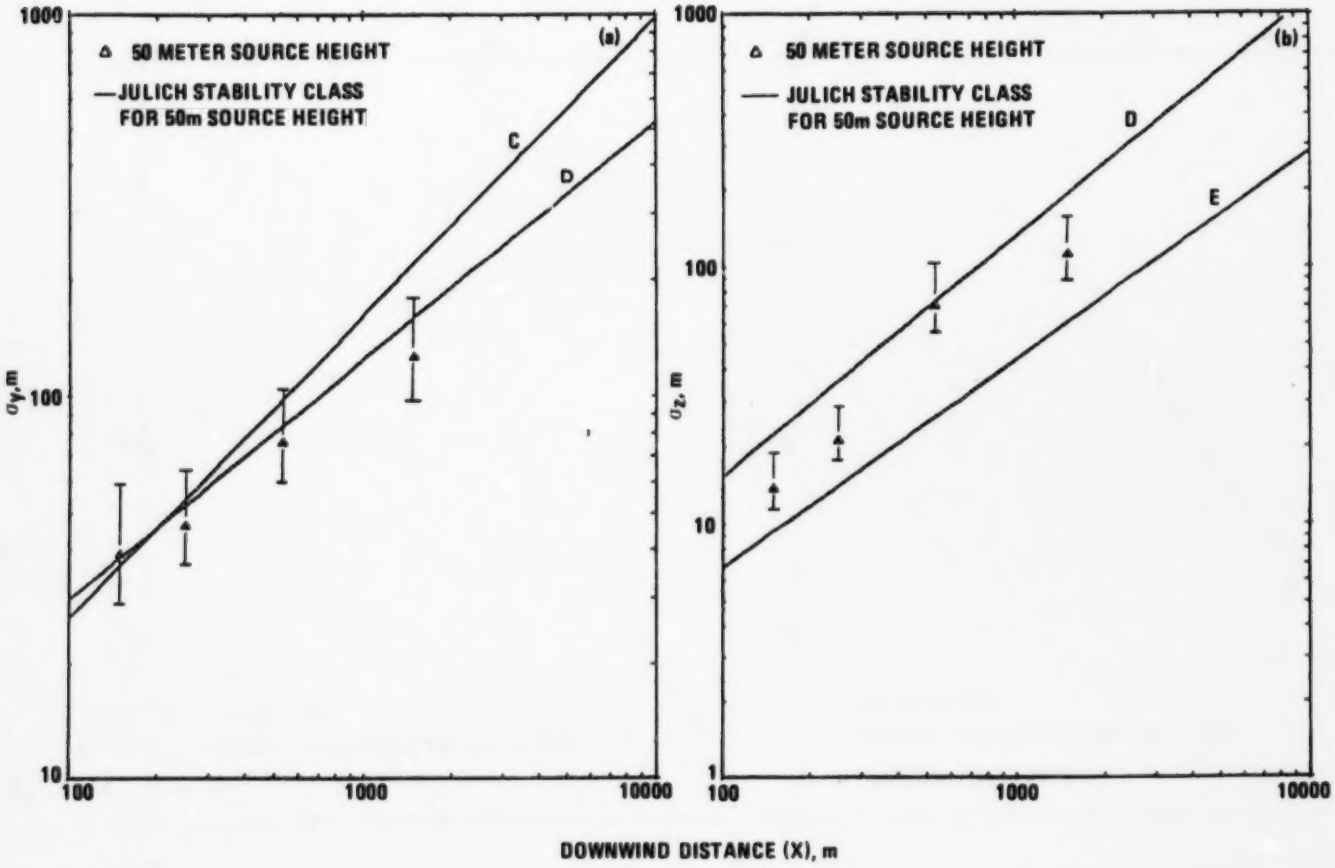

Figure 20. Dispersion coefficients compared with stability classes from the Julich study (Vogt, 1977) for 50 m source height; (a) lateral, (b) vertical.

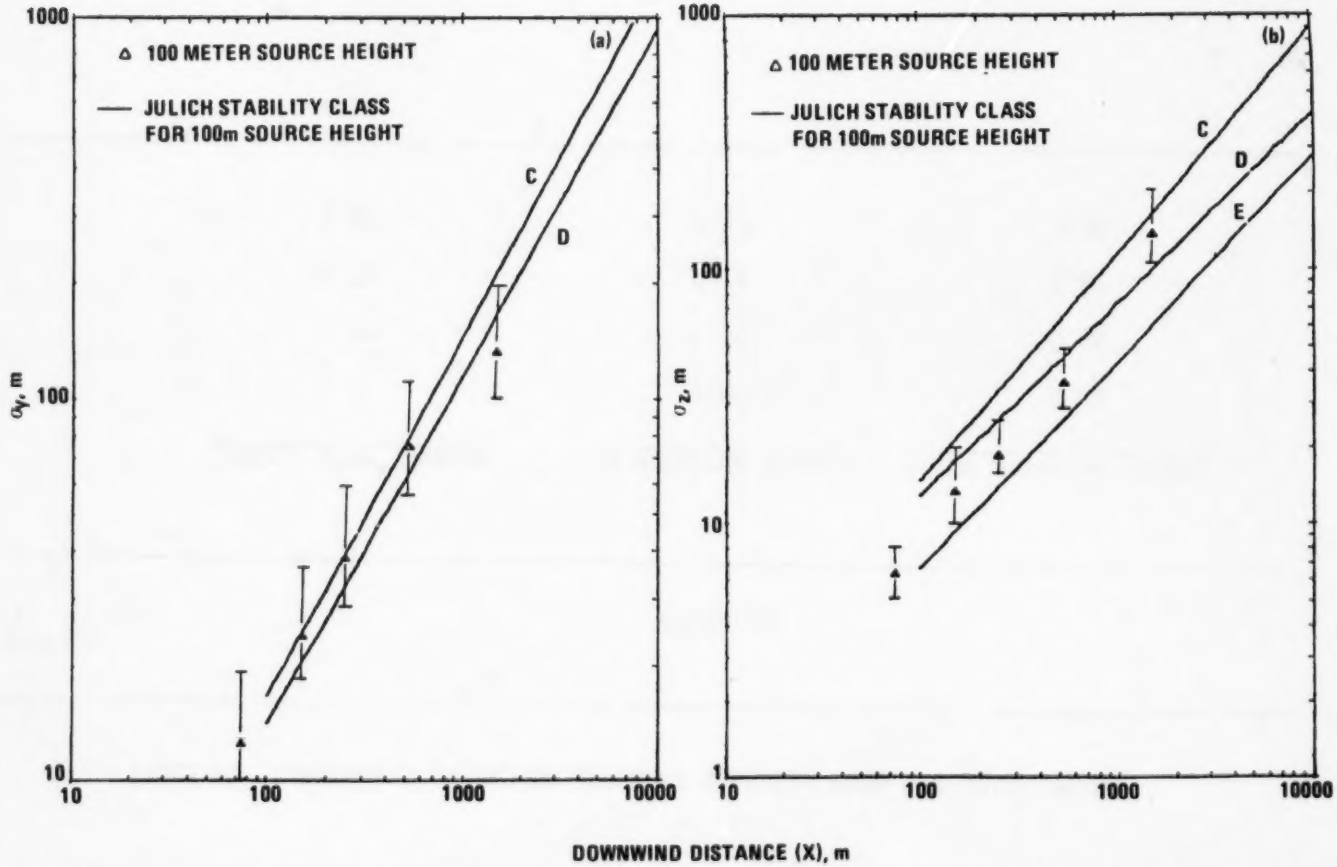

Figure 21. Dispersion coefficients compared with stability classes from the Julich study (Vogt, 1977) for 100 m source height; (a) lateral, (b) vertical.

TABLE 4. CONTINUITY CHECKS ON EFFLUENT RELEASES FROM THE STACK MODEL

Distance Downstream from Source (m, in MWT)	$C\int dydz/Q$		
	Ground Level Source	50 m Source Height	100 m Source Height
0.25	1.31	1.02	0.85
0.50	1.22	0.90	0.86
0.86	1.11	0.78	0.82
1.77	1.20	0.83	0.88

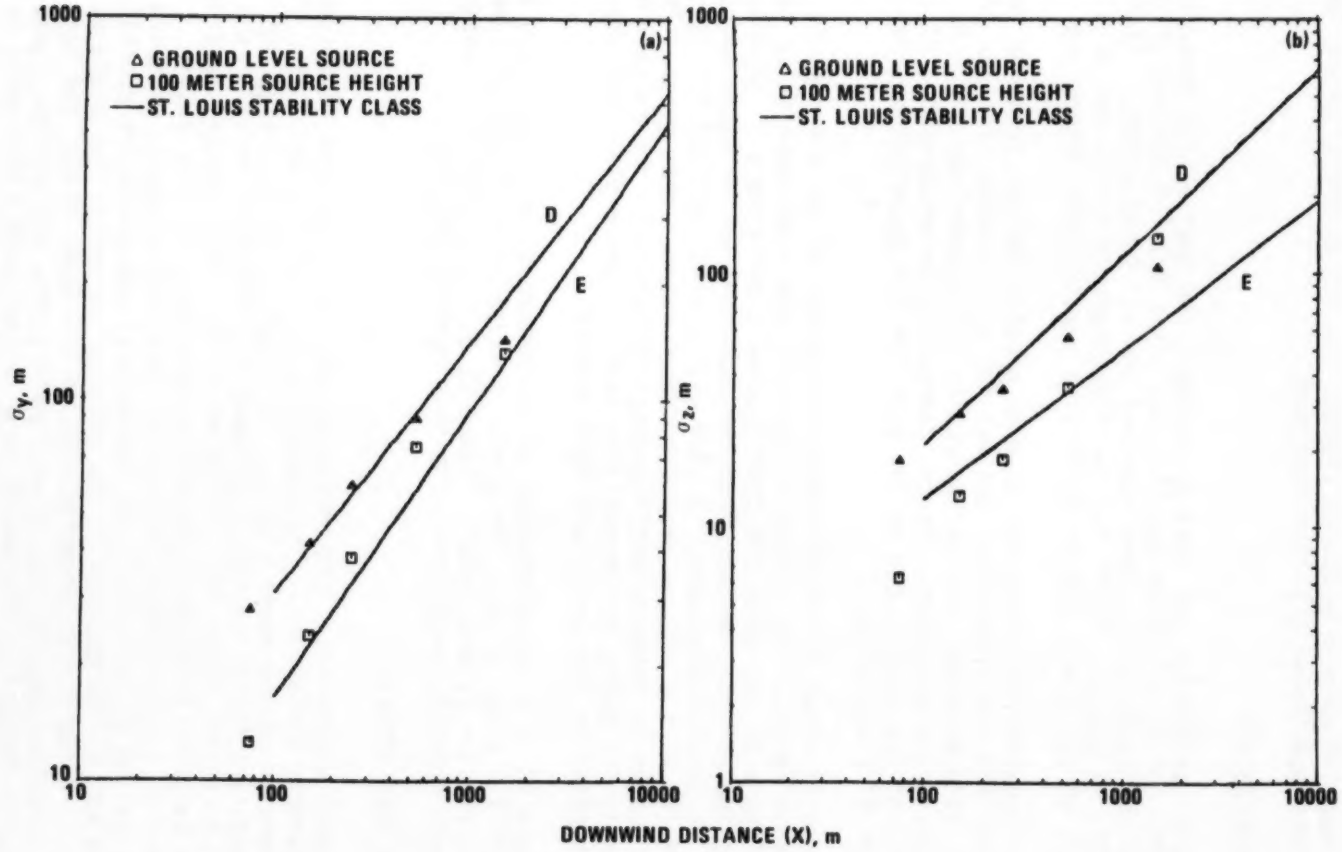

Figure 22. Dispersion coefficients for ground level and 100 m source heights compared with stability classes from the St. Louis study (McElroy, 1969).

layer has been simulated. Considerable confidence can be placed on the subsequent work concerning the wakes downwind of the standard design nuclear power plants since differences with and without the plants are of prime importance and absolute magnitudes are less important.

FLOW VISUALIZATION

Flow visualization was used to evaluate the qualitative features of the dispersion, and to determine sampling positions for the concentration measurements. Plume trajectories were examined for all three models, STACK, SNUPPS, and STRIDE. A general "feel" for the flow characteristics was acquired during this phase of the study, but no definitive results were determined.

The visualization study was used to provide insight into the gross features associated with the dispersion, but was not used to make detailed inferences. Lighting, film exposure, and smoke density differences can make the same situation appear quite different. Hence, concentration measurements of a tracer released from the source were relied upon for the quantitative evaluation and comparison of dispersion.

Figure 23 shows an instantaneous photograph of the STACK model for the 50 m release height. The plumes filled only the lower portion of the boundary layer. Figure 24 (a) shows the SNUPPS power plant with a 0° incident wind angle and the effluent release from the auxiliary boiler stack being swept downwind in the building wake. A view with a wind angle of 90° is shown in Figure 24 (b) with a release from the diesel exhaust vent stack. The plume does not appear to disperse until contact is made with the reactor building. The plume is following the streamlines over the power plant and then quickly being dispersed in the cavity and wake regions.

Figure 25 is a representation of instantaneous and time-lapse photographs for the STRIDE power plant. The plant is oriented at 0° and effluent released from both reactor island vents. Figure 25 (b) is a good representation of the entire wake envelope associated with this release situation.

BUILDING WAKE EFFECTS

Lateral and vertical concentration profiles were used to determine the plume standard deviations. The concentration profiles were taken at four locations downwind of the power plants. The complicated nature of the flow in the cavity adjacent to the buildings allowed only the data taken at the three most downwind locations to be used in the analysis. Thus insufficient data very near the building complexes proscribed inferences in this region. The vertical concentration profiles were obtained at locations directly downwind of the stack releasing the effluent, and the lateral concentration profiles were taken at the height of the maximum in the vertical concentration profiles. When the stack was located on the downwind edge of the power plant, the lack of influence of turbulent mixing made an extremely strong and narrow plume. A plume from a stack located on the upwind edge of the power plant would be mixed throughout the cavity region. These effects resulted in extremely large variations of the calculated plume standard deviations for the measurements near the power plants. These effects were not prevalent in the three downwind measurements which were used in the analysis.

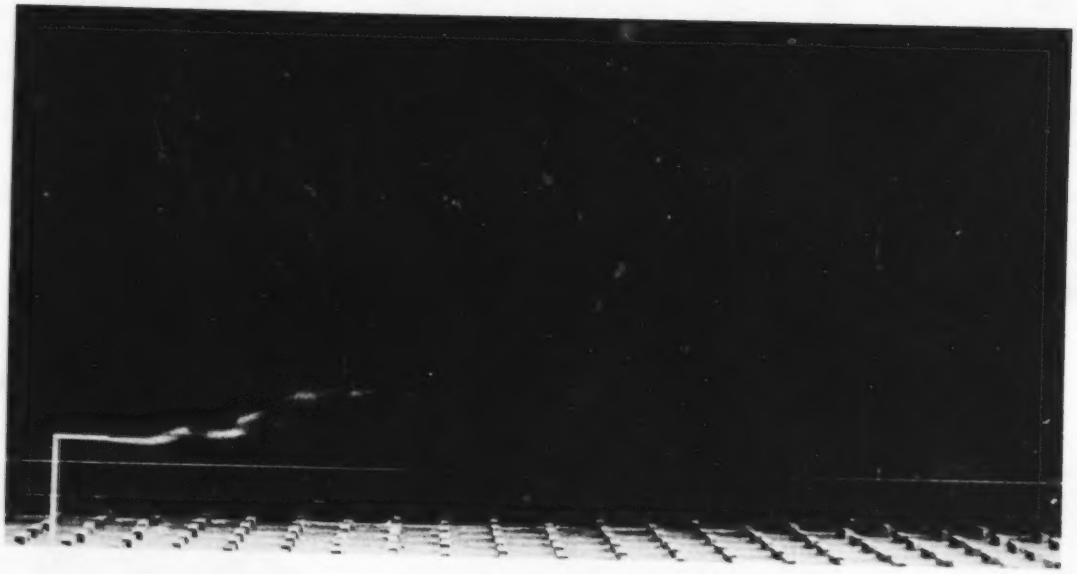

Figure 23. Instantaneous photograph of the STACK model with a 50 m release height.

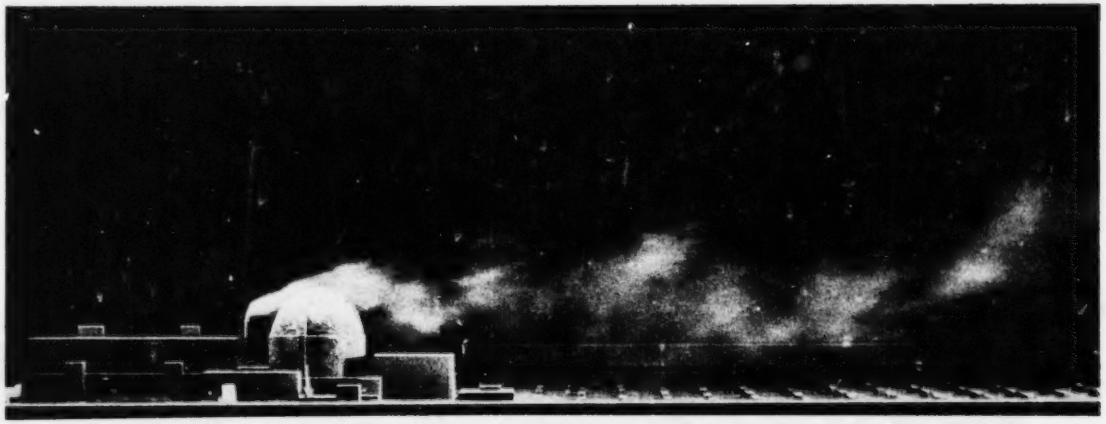

(a) ABS for 0° wind angle

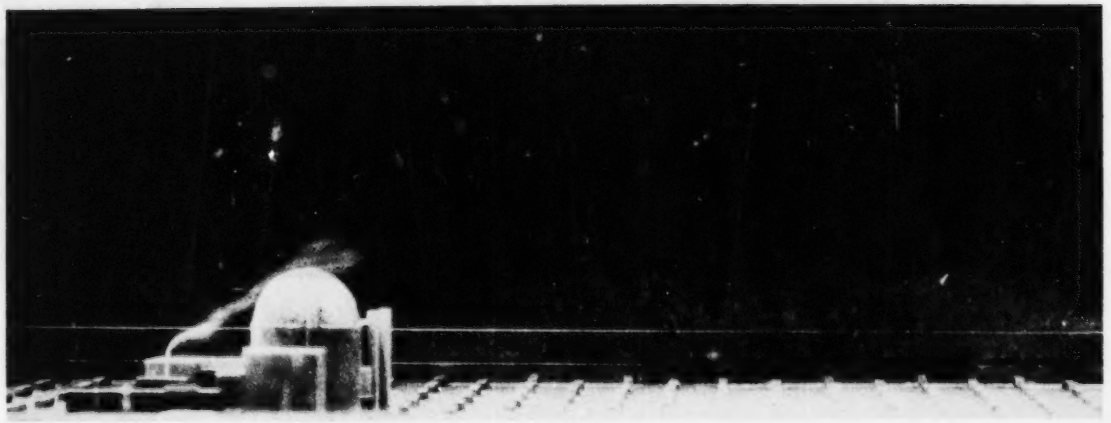

(b) DEV for 90° wind angle

Figure 24. Photographs of releases from the SNUPPS model.

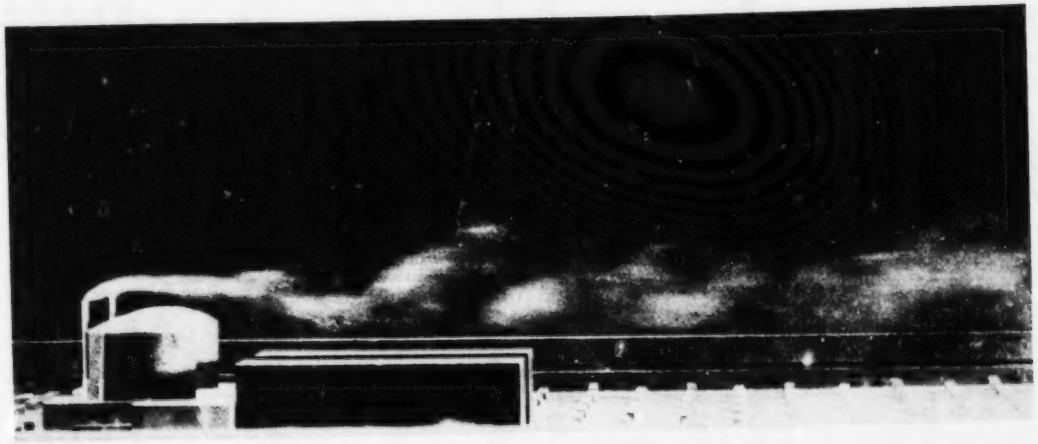

(a) instantaneous

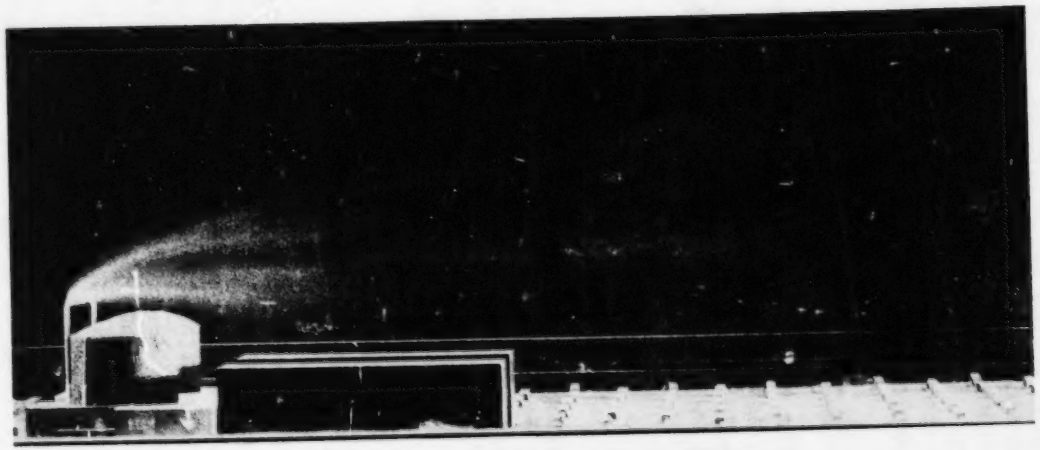

(b) 10-sec continuous exposure

Figure 25. Photographs of releases from the STRIDE model RIV for 0° incident wind angle.

The analysis consisted of applying a linear least squares fit to the plume standard deviations for each specific release situation or appropriate group of situations. A slope and intercept were determined for each release case. Each calculated slope and intercept described a function that represented the plume spread associated with the specific release situation. The functions were compared with the techniques as set forth in Regulatory Guide 1.111 (1977) of the U.S. NRC.

Wake functions were examined for effects associated with different incident wind angles and different stack releases for each power plant. It was determined that the major effects on the wake functions were associated with the incident wind angle and not the different stacks associated with the power plants. This is not to say that there are no effects due to stack position, which there undoubtedly are (Thompson and Lombardi, 1977). However, because of the complex structure of the power plants studied, these effects are minimal.

Building Wake Corrections

The NRC allows an adjustment for the vertical standard deviation for ground level releases of an effluent plume released within the building wake. This adjustment is an adaptation of work done by Yanskey, Markee, and Richter (1966), who applied a corrected standard deviation, Σ, in the form of

$$\Sigma = (\sigma^2 + \frac{A}{2\pi})^{\frac{1}{2}}$$

for measurements beyond 100 meters. The NRC has modified the method of Yanskey et al. in Regulatory Guide 1.111 (1977). For ground-level releases of the effluent plume within the building wake, Regulatory Guide 1.111 recommends the use of

$$\Sigma = (\sigma_z^2 + \frac{h^2}{2\pi})^{\frac{1}{2}}$$

if $\Sigma \leq \sqrt{3}\,\sigma_z$, otherwise $\Sigma = \sqrt{3}\,\sigma_z$.

Figures 26 and 27 are plots of Pasquill-Gifford stability classes corrected using the NRC method as applied to the SNUPPS power plant. The Pasquill-Gifford functions are those most commonly applied to full-scale data. The NRC wake correction without the restriction that $\Sigma = \sqrt{3}\,\sigma$ for values of $\Sigma > \sqrt{3}\,\sigma$ is also shown and is labeled unrestricted wake correction. The NRC wake correction causes a maximum increase in dispersion of approximately one stability class. It is asymptotic to the Pasquill-Gifford curves at large distances. For the unrestricted wake correction, very large increases in dispersion are associated with distances close to the power plants. The restriction is based on limited tracer studies by Dickson et al (1969) which showed an average dilution ratio of 3 for undisturbed flow versus disturbed flow.

Building Wake Functions for the SNUPPS and STRIDE Power Plants

For the SNUPPS model, the lateral and vertical building wake functions associated with the different incident wind angles are displayed in Figure 28.

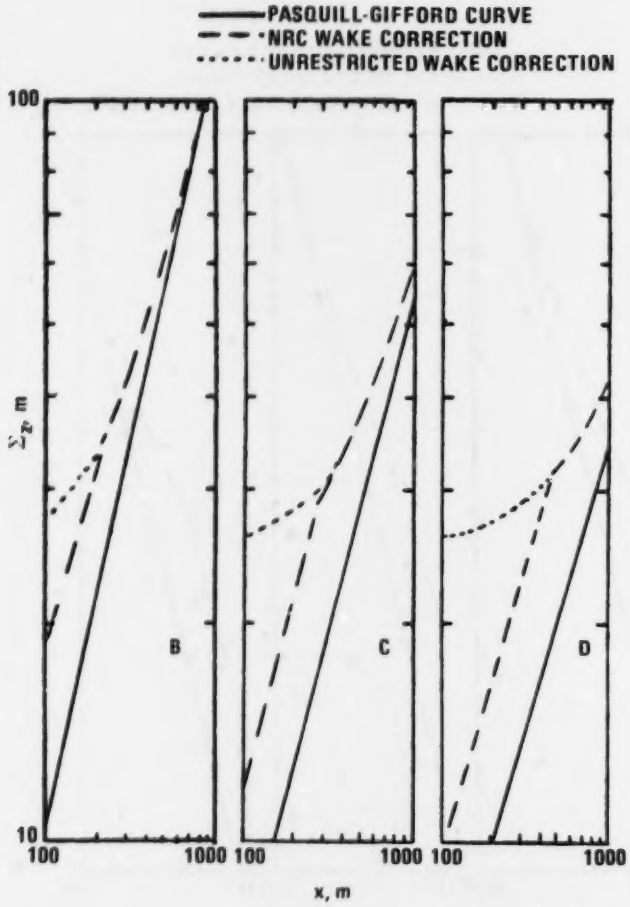

Figure 26. Pasquill-Gifford vertical stability classes plotted with the NRC building wake correction (NRC Reg. Guide 1.111, 1977) and the "unrestricted" wake correction for the SNUPPS plant.

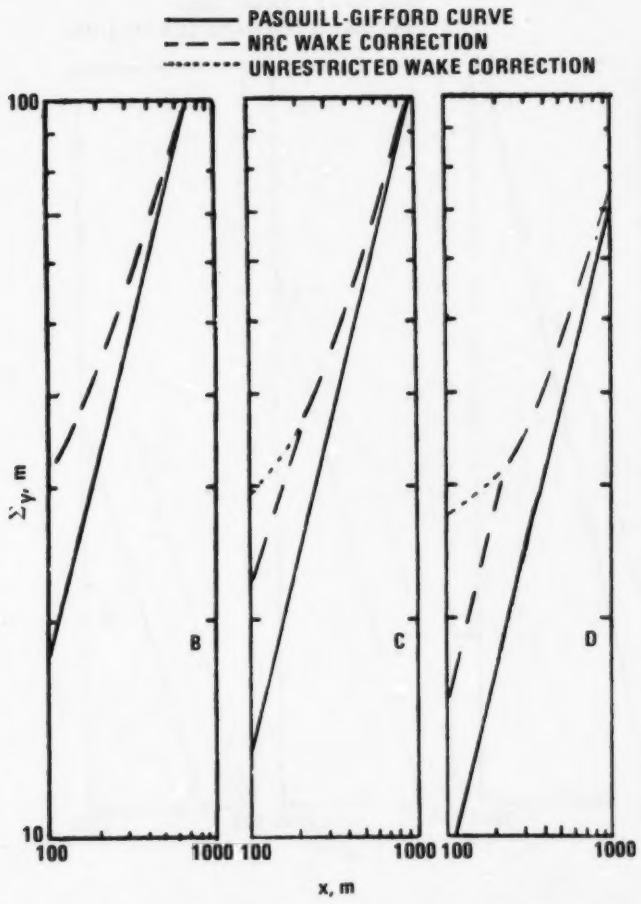

Figure 27. Pasquill-Gifford lateral stability classes plotted with NRC building wake correction (NRC Reg. Guide 1.111, 1977) and "unrestricted" wake correction for the SNUPPS plant.

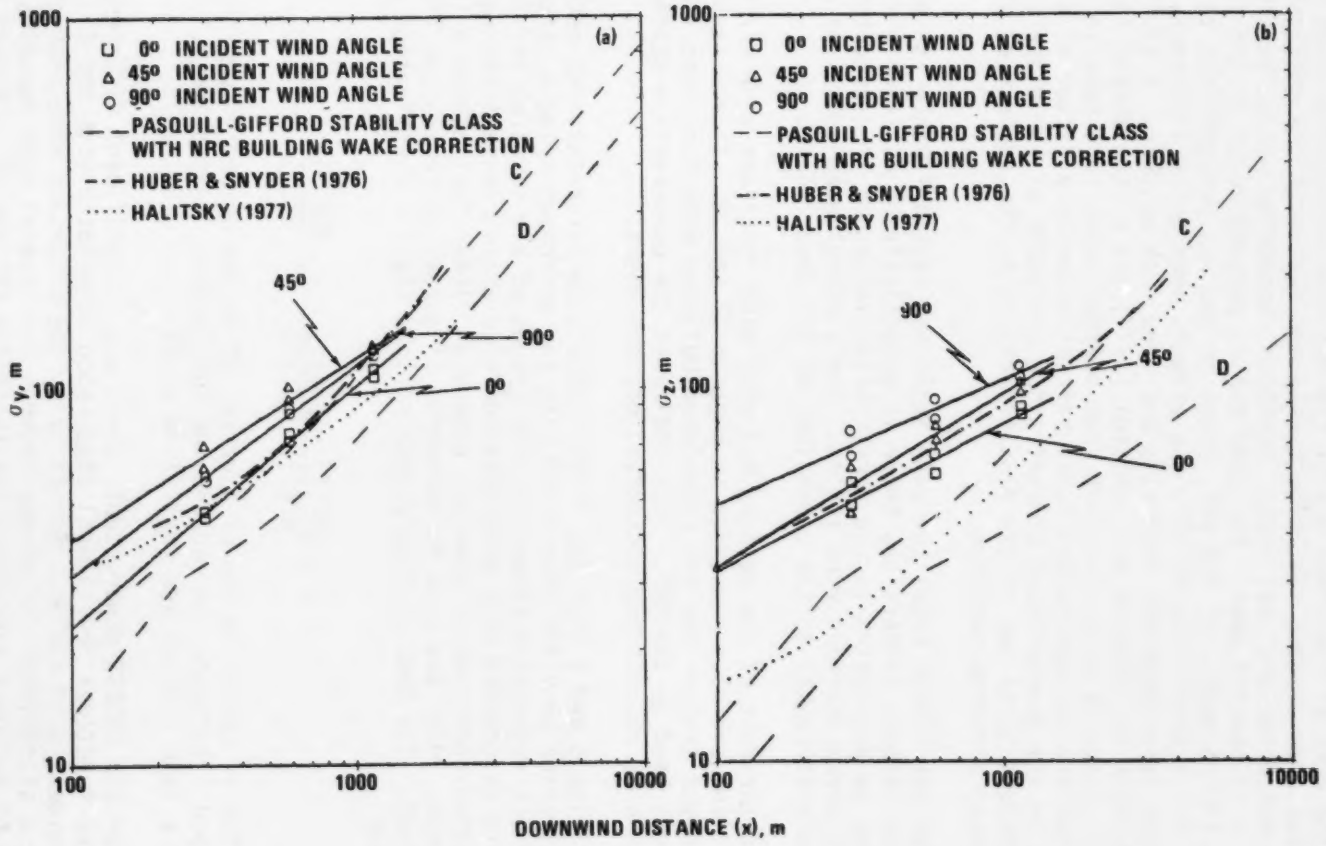

Figure 28. Building wake functions for the SNUPPS model; (a) lateral, (b) vertical.

Lateral dispersion indicated a direct relationship with the silhouette or projected area of the power plant; the building orientation with the largest projected area created the largest wake and that with the smallest projected area created the smallest wake. Vertical dispersion was at best weakly related to silhouette area. For wind angles perpendicular to the major axes of the SNUPPS model, 0° and 90°, plume spread was proportional to projected area. For a wind angle of 45°, the effects were quite different. The wake exhibited less spreading initially but grew much quicker. A similar finding was reported by Thompson and Lombardi (1977) for a cube shaped structure where a change in wind direction from perpendicular to a face to 45° to a face increased the maximum ground-level concentration by a factor of six. The increase in the ground-level concentration and width of the dispersion envelope were thought to be due to the flow separating at the corners of the building to produce standing vortices.

For the STRIDE model the wind angle had less influence as shown in Figure 29. For lateral dispersion, there is essentially no difference in plume spread. This may be attributed to the very similar values of projected building area for all three incident wind angles. The vertical wake functions were not related significantly to the dimensions of the power plant.

Comparisons of the derived building wake functions with the NRC wake corrections are also presented in Figures 28 and 29. In all cases, the dispersion was greater for the calculated building wake functions than for the functions used by the NRC. This indicates the conservative approach taken by the NRC when calculating concentrations and doses.

Tables 5 and 6 list the linear regression parameters for each set of concentration profiles associated with the different release situations. Also listed are regression parameters for groups of all vertical and lateral data, and data associated with each incident wind angle. With these data and the associated error sum of squares, a general linear test approach (Neter and Wasserman, 1974) was used to determine if groups of regression lines were identical. The test statistic used follows the F - distribution and has the form

$$F = \frac{SSE(R) - SSE(F)}{df(R) - df(F)} \div \frac{SSE(F)}{df(F)}$$

where SSE is the error sum of squares, df is the number of degrees of freedom, and R and F indicate the reduced and full models, respectively. The risk of making a Type I Error was controlled at 5%.

For the SNUPPS power plant, there was a significant difference between the wake functions for lateral dispersion associated with the 0°, 45°, and 90° incident wind angles. Scrutinizing the situation more thoroughly revealed a significant difference between the lateral wake function associated with a 0° incident wind angle and those for 45° and 90°. A test between the 45° and 90° wind angles indicated no significant difference. Figure 28(a) supports the above results.

For vertical dispersion associated with the SNUPP power plant, no significant difference was found to exist between the three wind angles or between

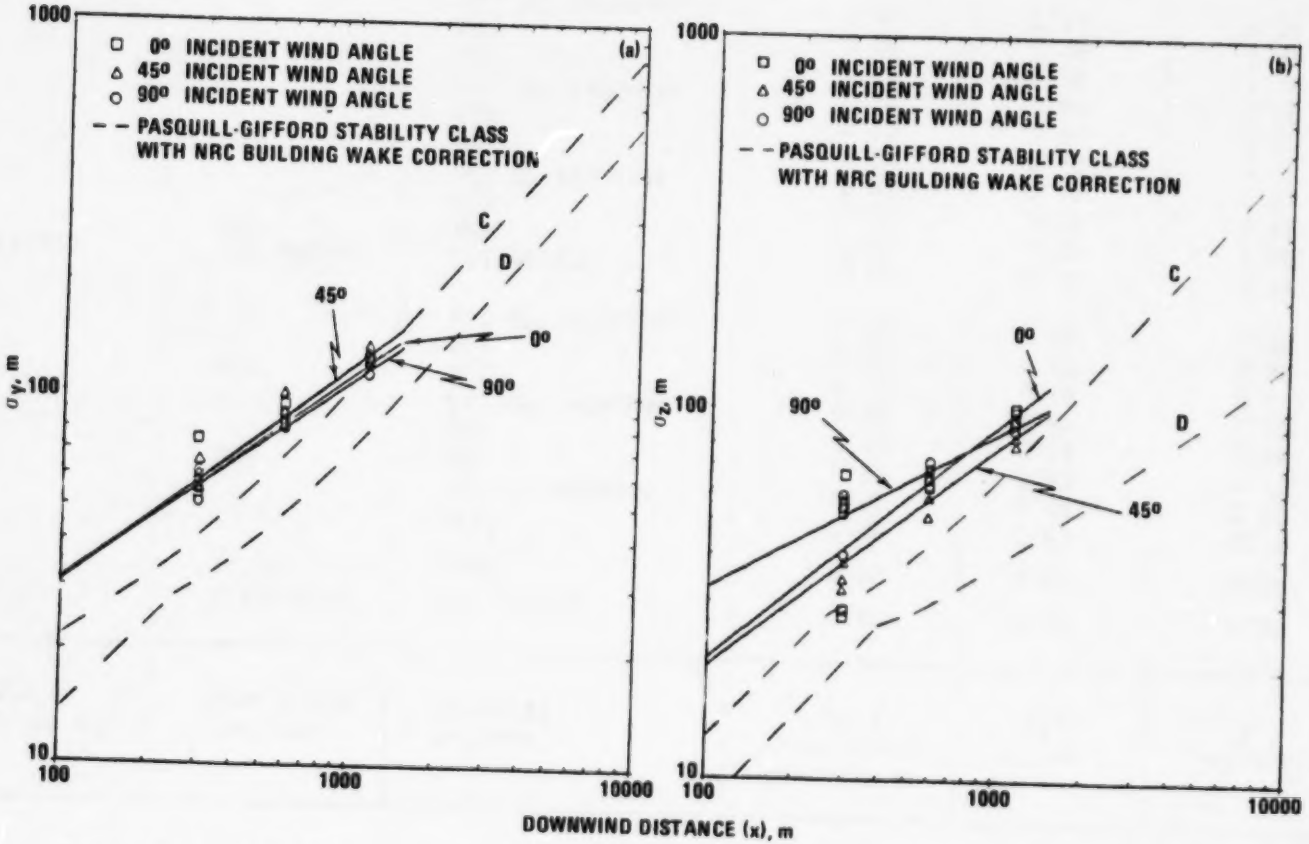

Figure 29. Building wake functions for the STRIDE model; (a) lateral, (b) vertical.

TABLE 5. REGRESSION PARAMETERS FOR A PLOT OF LOG_{10} (σ) VERSUS LOG_{10} (DISTANCE DOWNWIND) FOR THE SNUPPS MODEL

Direction of Dispersion	Incident Wind Angle	Release Point(s)	Correlation Coefficient (R^2)	Slope (B_1)	Intercept (B_o)
Lateral	All angles	All points	0.87	0.56	0.36
	0°	ABS[a]	0.99	0.67	0.00
		DEV[b]	0.99	0.61	0.18
		All 0° releases	0.99	0.64	0.09
	45°	ABS	0.98	0.43	0.79
		DEV	0.98	0.54	0.44
		All 45° releases	0.94	0.49	0.61
	90°	ABS	0.98	0.55	0.41
		DEV	0.99	0.57	0.35
		All 90° releases	0.98	0.56	0.38
Vertical	All angles	All points	0.65	0.40	0.77
	0°	ABS	0.87	0.30	1.02
		DEV	0.98	0.49	0.42
		All 0° releases	0.82	0.39	0.72
	45°	ABS	0.99	0.53	0.35
		DEV	0.98	0.40	0.82
		All 45° releases	0.82	0.47	0.58
	90°	ABS	0.99	0.29	1.16
		DEV	0.98	0.38	0.87
		All 90° releases	0.85	0.34	1.01

(a) ABS = auxiliary boiler stack

(b) DEV = diesel exhaust vent

TABLE 6. REGRESSION PARAMETERS FOR A PLOT OF LOG_{10} (σ) VERSUS LOG_{10} (DISTANCE DOWNWIND) FOR THE STRIDE MODEL

Direction of Dispersion	Incident Wind Angle	Release Point(s)	Correlation Coefficient (R^2)	Slope (B_1)	Intercept (B_o)
Lateral	All angles	All points	0.91	0.56	0.36
	0°	SGTV(1)[a]	0.99	0.71	-0.07
		SGTV(2)	0.90	0.29	1.16
		RIV(1)[b]	0.99	0.60	0.23
		RIV(2)	0.91	0.62	0.19
		All 0° releases	0.86	0.56	0.38
	45°	SGTV(1)	0.99	0.47	0.66
		SGTV(2)	0.97	0.55	0.45
		RIV(1)	0.99	0.62	0.18
		RIV(2)	0.99	0.68	0.02
		All 45° releases	0.92	0.59	0.30
	90°	SGTV(1)	0.99	0.52	0.50
		SGTV(2)	0.99	0.50	0.54
		RIV(1)	0.99	0.57	0.33
		RIV(2)	0.99	0.58	0.29
		All 90° releases	0.97	0.54	0.41
Vertical	All angles	All points	0.69	0.55	0.29
	0°	SGTV(1)	0.91	0.40	0.77
		SGTV(2)	0.91	0.94	-0.88
		RIV(1)	0.83	0.22	1.28
		RIV(2)	0.93	0.98	-0.94
		All 0° releases	0.96	0.54	0.21
Vertical	45°	SGTV(1)	0.96	0.54	0.21
		SGTV(2)	0.92	0.76	-0.34
		RIV(1)	0.75	0.28	1.04
		RIV(2)	0.96	0.79	-0.41
		All 45° releases	0.80	0.59	0.12
	90°	SGTV(1)	0.99	0.41	0.70
		SGTV(2)	0.90	0.32	0.95
		RIV(1)	0.81	0.32	0.96
		RIV(2)	0.95	0.63	0.08
		All 90° releases	0.85	0.42	0.67

(a) SGTV = standby gas treatment vent

(b) RIV = reactor island vent

any pair of incident wind angles. It should be noted that the agreement of 0° and 90° wind angles was quite close to being significant, as indicated by Figure 28(b).

For the STRIDE model, no wake function was significantly different from its cohorts for lateral or vertical dispersion.

Figures 30 and 31 are plots of intercept versus slope for the lateral and vertical dispersion associated with each individual release case for the SNUPPS and STRIDE models, respectively. A characteristic of all the plots of regression parameters is the linear relationship.

Figure 30 for the SNUPPS model is quite interesting. For lateral dispersion, there is a distinct relationship between the projected building area and the regression parameters. Building areas were assigned to the least squares fit to conform with values associated with the SNUPPS power plant. By selecting a projected building area in the ranges indicated on Figure 30(a), regression parameters that describe the wake region can be read directly from the figure.

The general linear tests to determine if groups of regression lines are identical are in direct agreement with Figures 30 and 31. In Figure 30(a), the 45° and 90° data are very closely related whereas the 0° data is somewhat segregated. For Figures 30(b), 31(a), and 31(b), there is no definite relationship between the regression parameters associated with the incident wind angles, as was also indicated in the statistical tests. These data imply a relationship between lateral wake characteristics and significant differences in projected building area.

Normalization of Derived Wake Functions

If the derived building wake functions could be adequately related to a physical aspect of their respective power plants, it might be possible to correlate standard deviations for any incident wind angle when specific wind direction data are known. This might be accomplished by normalizing just the standard deviation, σ, or both the standard deviation and the downwind distance, σ and x, respectively. Most normalizations were performed on the SNUPPS data because of the greater difference in wake function values.

Figure 32 normalizes the wake functions relative to the maximum building dimension in the direction of the dispersion. This technique met with little success. Figures 33(c) and (d) apply the square root of the projected building area as a normalizing parameter with considerably more success. Figure 33(c) has reasonably collapsed the data for lateral dispersion. A normalizing parameter of projected area is shown in Figures 33(a) and (b). These figures support the previous discussion relating plume spread to a function of building dimension.

Combining the SNUPPS and STRIDE wake functions helps to illustrate the overall success in normalizing laterally and the indequacy of normalizing vertically. Figure 33 shows the success accomplished for lateral normalization.

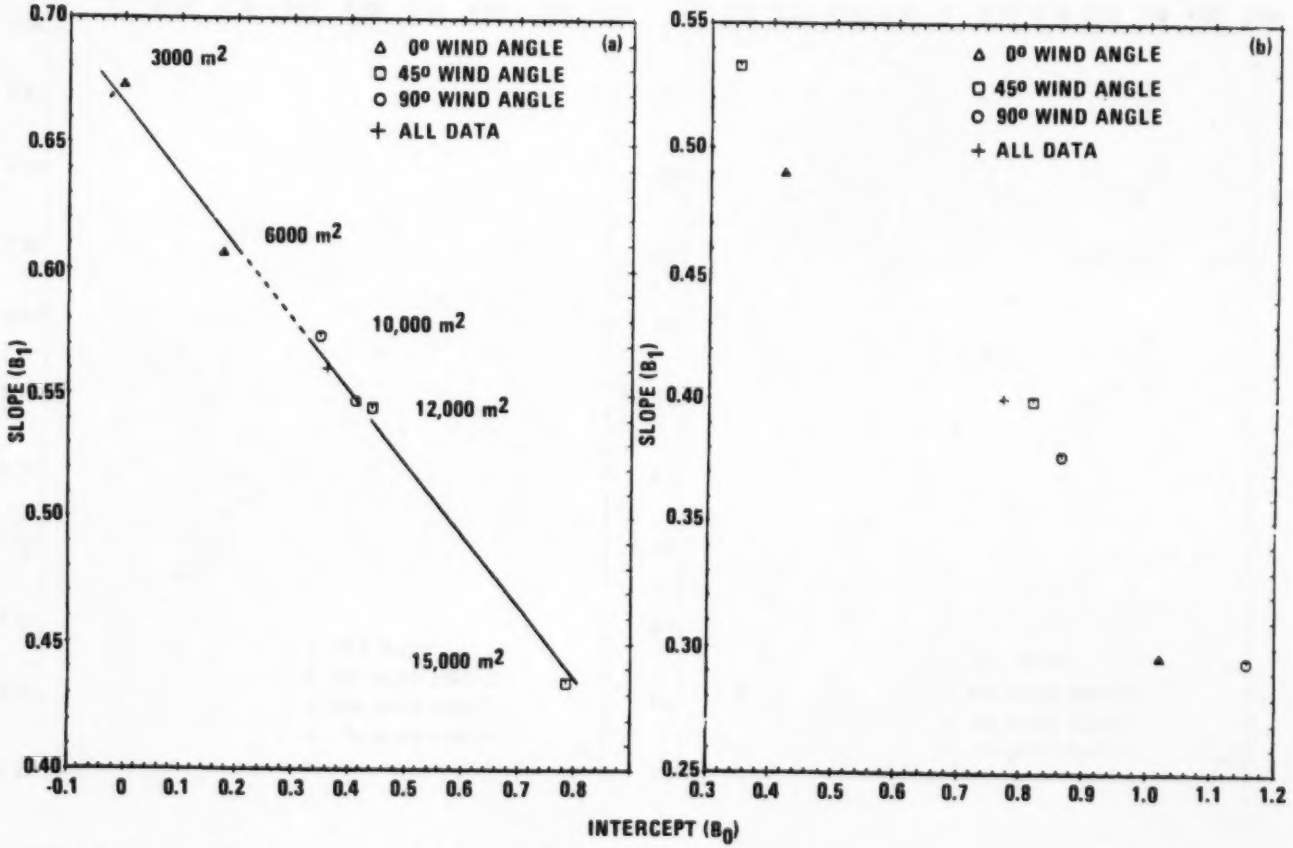

Figure 30. Wake functions for all SNUPPS release cases plotted by regression parameter; (a) lateral with estimated projected building areas, (b) vertical.

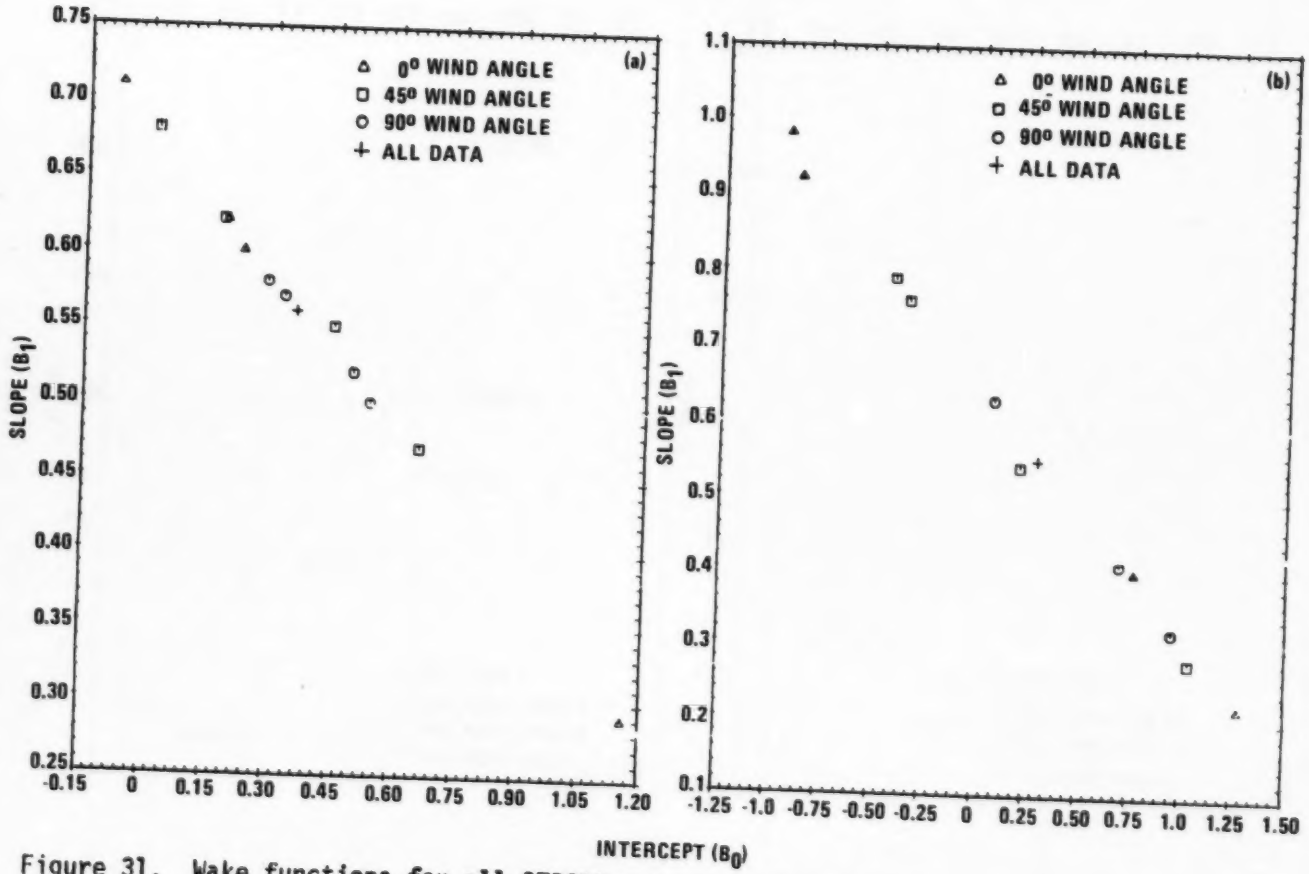

Figure 31. Wake functions for all STRIDE release cases plotted by regression parameter; (a) lateral, (b) vertical.

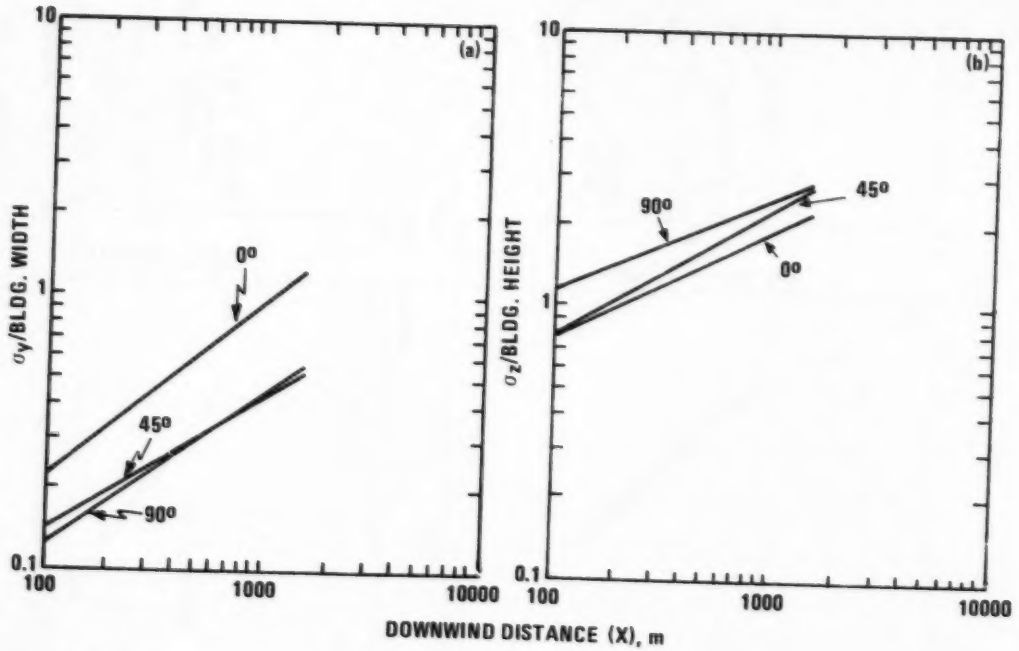

Figure 32. Wake functions for the SNUPPS model normalized by the maximum building width or height; (a) lateral, (b) vertical.

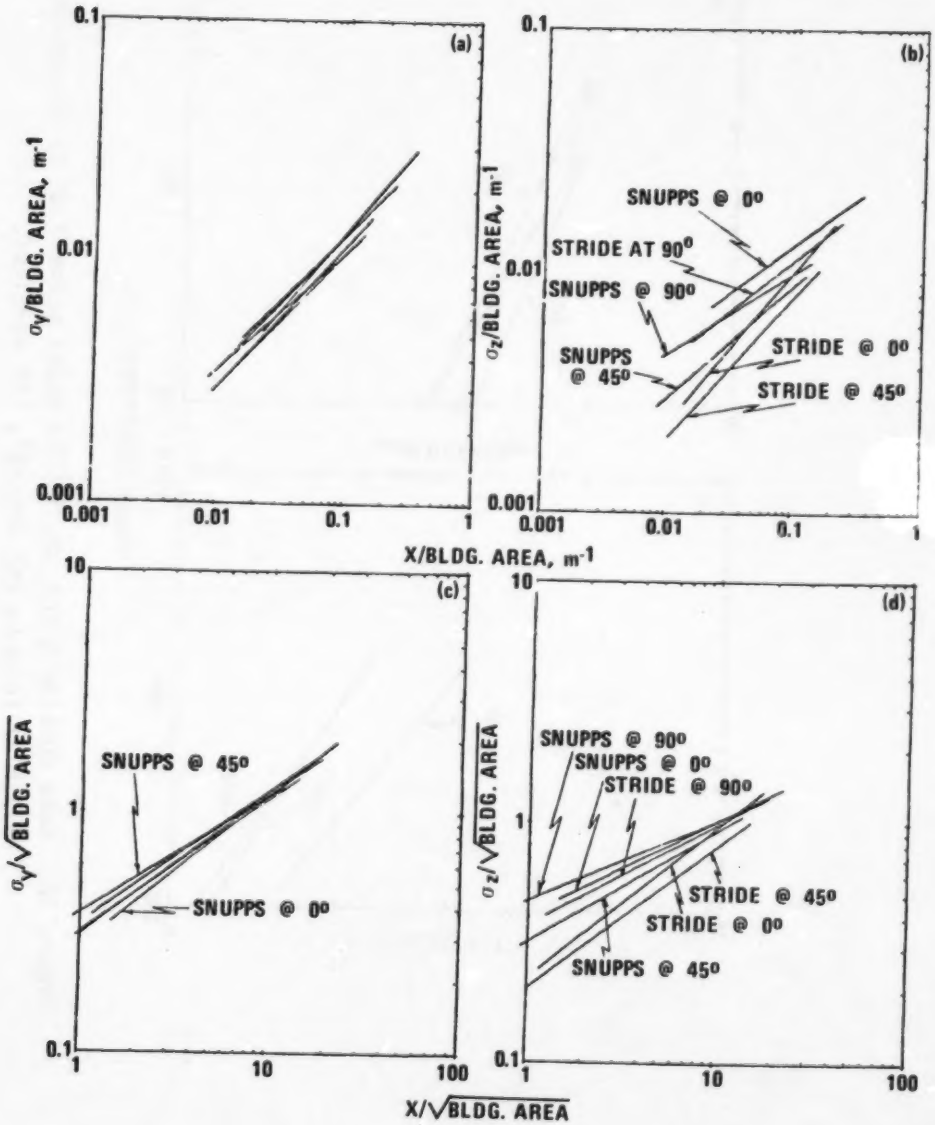

Figure 33. A comparison of SNUPPS and STRIDE wake functions: normalized by the projected building area; (a) lateral, (b) vertical and normalized by the square root of the projected building area; (c) lateral, (d) vertical.

For all projected areas associated with both models, the SNUPPS model at 45° and 0° represents the maximum and minimum, respectively. As might be expected, Figure 33(c) indicates the largest and smallest functional values to be those associated with the SNUPPS model at 45° and 0°, respectively. This corroborates the direct relationship between wake characteristics and projected building area for lateral dispersion. Vertical dispersion does not exhibit such characteristics.

REFERENCES

Castro, I.P., N.A. Jackson, and A.G. Robins. 1975. The Structure and Development of a 2 m Deep Simulated Suburban Boundary Layer. R/M/N 800, Marchwood Engineering Laboratory, Southampton, England.

Castro, I.P. and W.H. Snyder. Three Naturally Grown and Simulated Boundary Layers. Fluid Modeling Facility Internal Report, Environmental Protection Agency, Research Triangle Park, North Carolina, 200p.

Counihan, J. 1969. An Improved Method of Simulating an Atmospheric Boundary Layer in a Wind Tunnel. Atmospheric Environment, 3:197-214.

Counihan, J. 1975. Adiabatic Atmospheric Boundary Layers: A Review and Analysis of Data from the Period 1880-1972. Atmospheric Environment, 9:871-905.

Courtney, L. 1979. A Wind Tunnel Study of Flow and Diffusion Over a Two-Dimensional Low Hill. M.S. Thesis, N.C. State University, Raleigh, North Carolina, 134p.

Dickson, C.R., G.E. Start, and E.H. Markee, Jr. 1969. Aerodynamic Effects of the EBR-II Reactor Complex on Effluent Concentration. Nuclear Safety, 10:228-242.

Halitsky, J. 1977. Wake and Dispersion Models for the EBR-II Building Complex. Atmospheric Environment, 11:577-596.

Hoffman, F.O., D.L. Shaeffer, C.W. Miller, C.T. Garten, (eds.) 1978. Proceedings of a Workshop on the Evaluation of Models Used for the Environmental Assessment of Radionuclide Releases. Oak Ridge National Laboratory, Oak Ridge, Tennessee, CONF-770901.

Kaufman, J.W. 1977. Terrestrial Environment (Climatic) Criteria Guidelines for Use in Aerospace Vehicle Development, 1977 Revision. NASA Technical Memorandum 78118, National Aeronautics and Space Administration, November 1977.

Lettau, H. 1969. Note on Aerodynamic Roughness-Parameter Estimation on the Basis of Roughness - Element Description. J.A.M. 8:828-832.

Liu, H.T. and J.T. Liu. 1976. Plume Dispersion in Stably Stratified Flows Over Complex Terrain; Phase 2. EPA - 600/4-76-022. U.S. Environmental Protection Agency, Research Triangle Park, North Carolina.

McElroy, J.L. 1969. A Comparative Study of Urban and Rural Dispersion. J.A.M. 8:19-31.

Neter, J. and W. Wasserman. 1974. Applied Linear Statistical Models. Richard D. Irwin, Inc., Homewood, Illinois.

Regulatory Guide 1.111. 1977. Methods for Estimating Atmospheric Transport and Dispersion of Gaseous Effluents in Routine Releases from Light-Water-Cooled Reactors. U.S. Nuclear Regulatory Commission, Washington, D.C.

Robins, A.G. 1978. Plume Dispersion from Ground Level Sources in Simulated Atmospheric Boundary Layers. Atmospheric Environment 12:1033-1044.

Slade, D.H., (ed.) 1968. Meteorology and Atomic Energy. TID - 24190, U.S. Atomic Energy Commission.

Snyder, W.H. 1972. Similarity Criteria for the Application of Fluid Models to the Study of Air Pollution Meteorology. Boundary-Layer Meteorology 3:113-134.

Snyder, W.H. 1979. The EPA Meteorological Wind Tunnel: Its Design, Construction, and Operating Characteristics. EPA - 600/4-79-051, U.S. Environmental Protection Agency, Research Triangle Park, North Carolina.

Snyder, W.H. 1981. Guideline for Fluid Modeling of Atmospheric Diffusion. EPA - 600/8-81-009, U.S. Environmental Protection Agency, Research Triangle Park, North Carolina.

Snyder, W.H. and R.E. Lawson. 1976. Determination of a Necessary Height for a Stack Close to a Building - A Wind Tunnel Study. Atmospheric Environment 10:683-691.

Sutton, O.G. 1949. Atmospheric Turbulence. Methuen, 111p.

Thompson, R.S. and D.J. Lombardi. 1977. Dispersion of Roof-Top Emissions from Isolated Buildings - A Wind Tunnel Study. EPA - 600/4-77-006, U.S. Environmental Protection Agency, Research Triangle Park, North Carolina.

Turner, D.B. 1970. Workbook of Atmospheric Dispersion Estimates. Office of Air Programs, Pub. No. AP-26, U.S. Environmental Protection Agency, Research Triangle Park, North Carolina.

Vogt, K.J. 1977. Empirical Investigations of the Diffusion of Waste Air Plumes in the Atmosphere. Nuc. Tech. 34:43-57.

Wilson, D.J. and D.D.J. Netterville. 1978. Interaction of a Roof-Level Plume with a Downwind Building. Atmospheric Environment 12:1051-1059.

Yanskey, G.G., E.H. Markee, Jr., and A.P. Richter. 1966. Climatography of the National Reactor Testing Station. IDO-12048, Idaho Operations Office, U.S. Atomic Energy Commission.

U.S. ENVIRONMENTAL PROTECTION AGENCY
Office of Research and Development
Center for Environmental Research Information
Cincinnati, Ohio 45268

OFFICIAL BUSINESS
PENALTY FOR PRIVATE USE. $300
AN EQUAL OPPORTUNITY EMPLOYER

POSTAGE AND FEES PAID
U.S. ENVIRONMENTAL PROTECTION AGENCY
EPA-335

If your address is incorrect, please change on the above label tear off; and return to the above address.
If you do not desire to continue receiving these technical reports, CHECK HERE ☐; tear off label, and return it to the above address,

5/5
8447